Civil Engineering Graduate Theses & Dissertations   Civil, Environmental, and Architectural Engineering

Spring 1-1-2014

The Effect of Temperature on Moisture Transfer in Concrete

Yao Wang
University of Colorado at Boulder, Yao.Wang-1@colorado.edu

THE EFFECT OF TEMPERTAURE ON MOISTURE TRANSFER IN CONCRETE

By

YAO WANG

B.S., Taiyuan University of Technology, 2012

A thesis submitted to the

Faculty of the Graduate School of the

University of Colorado in Partial Fulfillment of the requirement for the degree of

Master of Science

Department of Civil, Environmental and Architectural Engineering

2014

This Thesis entitled:

The Effect of Temperature on Moisture Transfer in Concrete

Written by Yao Wang

Has been approved for the
Department of Civil, Environmental and Architectural Engineering

_____

Yunping Xi

_____

George Hearn

_____

Petros Sideris

Date_____

The final copy of this thesis has been examined by the signatories, and we find that
both the content and the form meet acceptable presentation standards of scholarly
work in the above mentioned discipline

Yao Wang (M.S., Civil, Environmental and Architectural Engineering)

The Effect of Temperature on Moisture Transfer in Concrete

Thesis directed by Professor Yunping Xi

This thesis presents results of an experimental investigation of how the temperature gradient affects the moisture in concrete.

The thesis includes two major parts. The first part introduces the background information as well as the theoretical review which includes theory definition and formula derivation.

The second major part includes the development of the experimental setup, analysis of the results and formulation of the governing equation to characterize the moisture and temperature coupling effect. The investigational and numerical results in this section are used to validate assumptions made about how the temperature gradient affects the moisture transfer in concrete.

ACKNOWLEDGMENT

I would like to express my deep appreciation and thanks to my advisor Professor Yunping Xi for his guidance, support and patience throughout the whole period. His fruitful academic suggestions and valuable innovative ideas have always been encouraging and have been guiding my research until completion.

I would also like to thank Professor Bazant. He has summarized some effective theory and equations about the coupled heat and moisture transfer in concrete which gave me the support and guidance to help me be familiar with the coupling effect of moisture and temperature in concrete.

I would like to thank my committee members: Professor George Hearn and Professor Petros Siders. Thanks for your helpful suggestions and attendance of my final thesis.

I would like to extend my appreciation to my parents, my wife, my younger sister and whole family for their love and encouragement without which this work would have never been accomplished successfully.

TABLE OF CONTENTS

LIST OF FIGURES

LIST OF TABLES

CHAPTER 1

INTRODCUTION

1.1 Background

The transport of moisture in concrete is of a major concern in predicting the long-term performance of reinforced concrete structures such as buildings and bridges. The transport of moisture in concrete can cause the following durability and serviceability problems (Zhong, Z. et al [2008]):

1. Volume changes (swelling, warping and shrinkage) that can cause cracking, etc.;

2. Freeze-thaw deterioration of concrete;

3. Discoloration of building finishes;

4. The growth of biological forms, including molds, mildews, mites, etc.

5. Corrosion of metal components, such as reinforcement bars, HVAC equipment, etc.;

In order to understand the durability and serviceability problems of concrete structures, it is necessary to predict accurately and reliably the moisture transfer process in concrete.

1.2 Objectives of the Thesis

Under an isotherm condition, the moisture flux, J, can be considered to be proportional to the gradient of moisture concentration. The equation is shown as follows:

$$J = -\frac{a}{g}\ grad\ p \qquad\qquad eq\ (1.1)$$

in which J is the moisture flux, a is permeability, g is gravity acceleration (m/s^2), and p is pore vapor pressure (Bazant, Z.P. [1978]).

When moisture transfer takes place not under the isotherm condition, the contribution of the temperature to moisture transfer must be taken into account, which is called the Soret effect (Platten, J.K. [2006]). In this case the moisture flux is not only related to the gradient of moisture concentration but also related to the temperature gradient. Therefore, an objective of this thesis is to evaluate how the temperature gradient affects the moisture transport in concrete.

In this study, an experimental setup was developed to investigate the coupling effect, the effect of temperature gradient on moisture transfer in concrete. The temperature gradient in concrete sample was the independent variable in the experimental study. Governing equations for the moisture transfer under the influence of a thermal gradient were developed. The coupling effect is represented in the governing equation by a coupling parameter. By using the governing equation and the experimental results, it is possible to study the coupling effect and determine the coupling parameter.

1.3 Organization of the Thesis

There are five chapters in the thesis. The current chapter introduces the background information and the objective of the thesis. The remaining chapters are organized as follows:

Chapter 2 presents a literature review explaining the basic transport mechanics in concrete, and the relationship between the temperature gradient and moisture flux in concrete. This chapter introduces a model study about the high temperature affecting the moisture transfer in concrete.

Chapter 3 derives the governing equations for the coupling effect of moisture and temperature. The basic assumptions for the governing equation are discussed and explained in detail.

Chapter 4 discusses the experiment details including the purpose, procedures and results. The final results are discussed and the assumptions are validated.

Chapter 5 contains the conclusions of the present study and recommendations for further research.

CHAPTER 2

LITERATURE REVIEW

Moisture movement in concrete under the influence of a thermal gradient is one of the main concerns of the durability and serviceability of concrete structures. This chapter presents a literature review of the topic.

2.1 Transport Mechanisms in Concrete

The transport properties of concrete are related to the quantity of transferring moisture and temperature through concrete. The movement of moisture including the liquid phase (water) and gas phase (vapor) through concrete can take place according to four major basic mechanisms: sorptivity, permeability, diffusivity and migration. Migration is the moisture transport due to electrical potential gradients, which is not the main focus of this thesis. The other three mechanisms are explained in detail in the following sections.

2.1.1 Sorptivity

Sorptivity occurs due to the capillary action inside void spaces of cement paste. An example of a water sorptivity test in concrete is displayed below (Han, B., et al. [2012]):
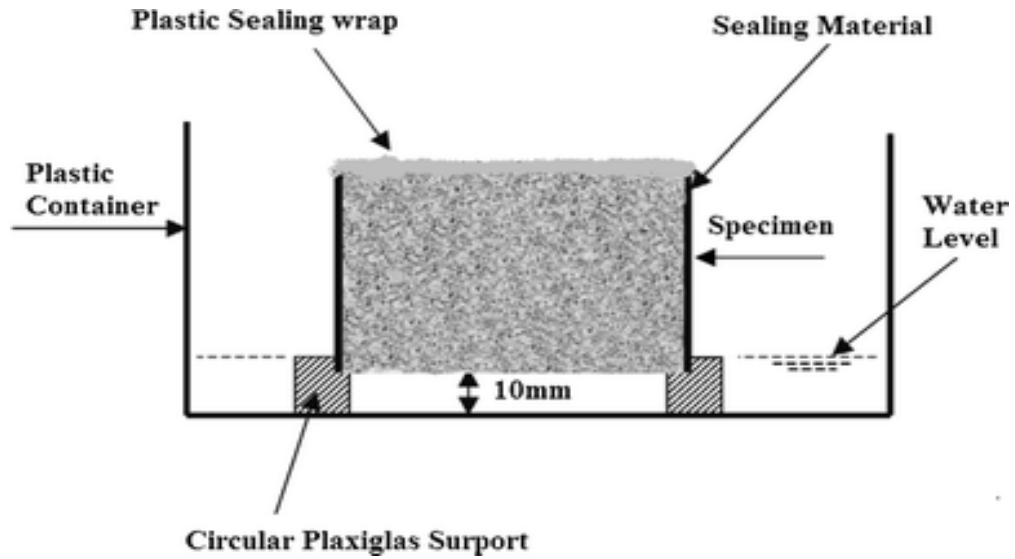
Figure 1 Sorptivity Experimental Setup

The specimen was cut from a $50 \times 50 \times 50$ mm cubic sample. The specimen was oven-dried at 105 ^{o}C for 24 hours and then placed in an environmental chamber at a temperature of 50 ± 2 ^{o}C and Relative Humidity of $80 \pm 3\%$ for three days to ensure that the initial moisture content in the concrete sample is uniformly distributed throughout the specimen. Afterward, the specimen was placed into a sealable container at 23 ± 2 ^{o}C for 15 days to allow a free flow of air around the specimen. The test was performed by allowing one sample surface (the bottom surface) to be in contact with water at a 10 mm depth using a circular Plexiglas support. Using the supporting frame and keeping the water level at 1-3 mm above the top of Plexiglas support allowed continuous contact between the specimen surface and the water without changing the water depth throughout the test. The weight of the specimen was measured at fixed time intervals. The increase of specimen weight comes from the amount of water absorbed by the concrete, which is an indication of the sorptivity of the concrete.

The significance of concrete sorptivity relies on a variety of factors, but the key aspect is the degree of aeration to which the samples have been exposed, which depends strongly on the concrete composition or concrete mix design parameters. The following relationship has been empirically derived from the analysis of experimental results to calculate the sorptivity coefficient (Han, B., et al. [2012]).

$$\frac{Q}{A} = k_s \sqrt{t} \qquad eq\ (2.1)$$

$where:$
$Q = the\ amount\ of\ water\ absorbed\ which\ could\ be\ got\ from\ the\ weight\ changing;\ (g)$
$A = the\ cross-sectional\ area\ of\ the\ specimen\ that\ was\ in\ contact\ wiht\ water;\ (cm^2)$
$t = time;\ (sec)$
$k_s = the\ sorptivity\ coefficient;\ (^g/_{m^2}\ for\ mass\ or\ {^{m^3}}/_{m^2}\ for\ volume\ )$

2.1.2 Permeability

Permeability is the flow rate of a fluid or gas through the concrete under a pressure gradient. Permeability is affected mainly by the porosity and the pore structure.

The porosity of a material equals to the ratio of the volume of all the pores to the whole volume of the material. In general, the higher the porosity is, the higher the permeability is. This is because porous space in concrete provides an easy pathway for the fluid to move around in the material. However, the porosity is not the only measure for the effect of porous space on the permeability of porous media. Pore structure plays an important role in addition to the porosity.

The pore structure is related to the pore size distribution, pore shape, tortuosity and connectivity of pores:

Pore size distribution affects the permeability. The larger the pores in the concrete, the easier the fluid will pass through the pores. This is related to the viscosity of the fluid and the surface force of pores. For example, the surface force in small pores can hold the flowing fluid and reduce the flow rate.

Pore shape is a factor affecting the transmittance because the irregular shape can impede the flow. For example, when pores are in laminar shape and arranged in parallel (e.g. in layered pore structure), it will be difficult for the fluid to flow through in the transverse direction.

Tortuosity is the ratio of actual pore length between two points and the projected length of the pore length between the two points. It is a measure of the degree of zigzag of a pore. Apparently, the higher the tortuosity is, the more difficult for a fluid flows through the pore.

Connectivity is important because if the pores are disconnected, the fluid will be blocked and cannot continue to move. Even with a large porosity, the permeability of a porous media could be low if the connectivity of pores is low.

A test about water permeability in concrete is shown below (Han, B., et al. [2012]):

The water permeability is measured through a falling head test. The concrete sample was cut from a $50 \times 50 \times 50$ mm cubic sample. Prior to the test, the sample was applied approximately 1 mmHg (133 MPa) in a clean dry vacuum desiccator for three hours. Deionized water was added to cover the sample for one more hour. Afterwards, the vacuum was turned off and the sample was left in the water for another 18 hours. Then, the specimen was removed from the desiccator and lightly patted with paper towel. After sealing the sides of the sample, the whole test setup was assembled and then tested. The

water drop was measured every 24 hours for the first week, then once every two days for the rest of the time. After each measurement, water was replenished to the original level to ensure the constant pressure gradient.
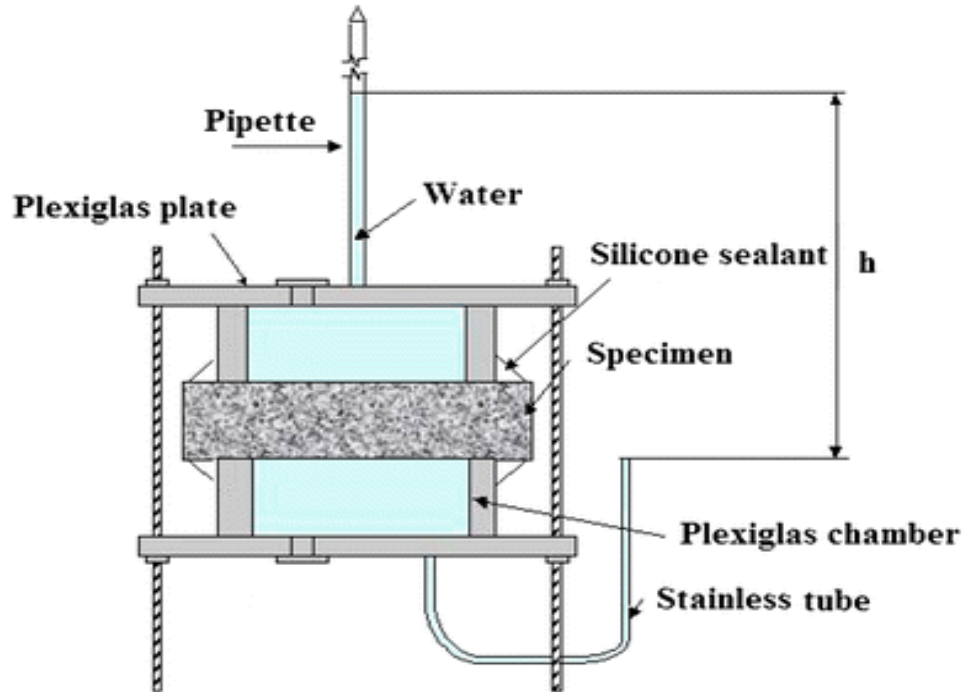
Figure 2 Permeability Experimental Setup

The water flow through the system is assumed to be continuous and laminar. Then the permeability coefficient can be derived from the Darcy's law:

$$k_f = \left(\frac{a \times l}{A \times t}\right) ln \left(\frac{h_i}{h_f}\right) \qquad eq(2.2)$$

$where$:
$k_f = the\ permeability\ coefficient;\ (^{cm}/_s)$
$A\ \ = the\ cross-sectional\ area\ of\ specimen;\ (cm^2)$
$a\ \ = the\ cross-sectional\ area\ of\ pipette;\ (cm^2)$
$l\ \ \ = the\ specimen\ thickness;\ (cm)$
$t\ \ \ = time;\ (sec)$
$h_i\ ,h_f = the\ inital\ and\ final\ water\ heads\ respectively;\ (cm)$

2.1.3 Diffusivity

Diffusivity is the measure of the ability for a chemical to transport in concrete.. The movement of chemical is from an area of higher concentration to an area of lower concentration. Diffusion has two conditions: stationary diffusion (steady state flow) and non-stationary diffusion (non-steady state flow) (Han, B., et al. [2012]).

Steady State Flow

Under the stationary condition, the process of diffusion can be described by Fick's first law:

$$J = -D\frac{\partial C}{\partial x} \qquad eq(2.3)$$

$where$:
$J = diffusion\ flux;\ \left(\dfrac{kg}{m^2 \times s}\right)$
$D = diffusion\ coefficient;\ \left(\dfrac{m^2}{s}\right)$
$\dfrac{\partial C}{\partial x} = concentration\ gradient;\ (\dfrac{kg}{m^4})$

Note: the diffusion coefficient depends on the diffusion of matter, characteristics of concrete and environmental conditions. This coefficient may not be a constant for concrete with the same mix design and it could be a function of position and time, due to variations in the pore structure, which may be caused by the applied service load on the structure or the environmental temperature or humidity. (Bertolini et al. [2004])

Non-Steady State Flow

Non-steady state flow normally occurs in concrete structures, while the steady state is rare. The process of diffusion under the non-steady condition can be described by the Fick's second law:

$$\frac{\partial C}{\partial t} = D \frac{\partial^2 C}{\partial x^2} \qquad\qquad eq(2.4)$$

Note: the above equation can be derived from Fick's First law and the mass conservation in absence of any chemical reactions:

$$\frac{\partial C}{\partial t} + \frac{\partial J}{\partial x} = 0 \rightarrow \frac{\partial C}{\partial t} - \frac{\partial}{\partial x}\left(D \frac{\partial C}{\partial x}\right) = 0 \qquad eq(2.5)$$

The equation 2.4 can be solved by assuming the following initial condition and boundary condition (which is a one dimension diffusion problem with a constant boundary and initial condition and a constant diffusivity):

Boundary condition: $C = C_s$ *for* $x = 0$ *and for any* t;

Initial condition: $\quad C = 0 \quad$ *for* $x > 0$ *and* $t = 0$;

Integrating under the assumptions, the solution is (the details are not provided here):

$$\frac{C}{C_s} = 1 - erf\left[\frac{x}{2\sqrt{D\,t}}\right] \qquad\qquad eq(2.6)$$

where:
C = *concentration at distance* x *from the concrete surface at time* t;
C_s = *surface concentration*;
erf = *error function*; *where*: $erf(z) = \frac{2}{\sqrt{\pi}} \int_0^z e^{-t^2}\, dt$

2.2 Theory of the Coupled Heat and Moisture Transport

Under the service condition, most of concrete structures are not under the isotherm state. Temperature variation and humidity fluctuation take place at the same time. Therefore, the coupling effects between heat transfer and moisture transport must be considered. Heat transfer is governed by Fourier's law (Szekeres, A. [2012]), and moisture transfer is governed by Fick's law, as described earlier. When both temperature and moisture are considered, the two laws need to be modified by including the coupling effects, which are defined by the Soret and Dufour effects. In the following sections, the heat transfer and moisture transport are described first as two individual transport processes in concrete, the corresponding basic governing equations are established; and then the coupling effects are introduced and included in the basic governing equations.

2.2.1 General Modes of Heat and Moisture Transport

Several modes of heat and moisture transport take place in a porous concrete structure surrounded by a moist air with the heat supplied by sunlight as shown in the sketch in the following figure.
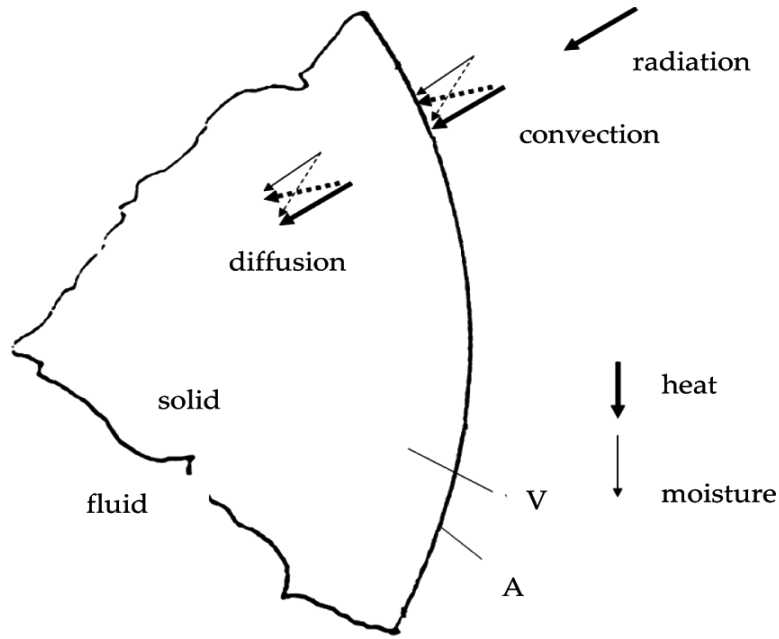
Figure 3 Modes and Objects of Transports

Diffusion of moisture occurs inside of the body, while convection of fluid and heat and radiation of heat occur on the boundary of the body. Moisture in this case is referred to a mixture of liquid water and water vapor. Therefore, the diffusion is the contact interaction between the diffusing agent (the water molecule in this case) and the solid frame of pore wall, while the convection is the interaction between the solid and water or the solid and the heat. The radiation embodies a remote interaction of the concrete and sunlight.

The following two tables summarize the transport feature of heat and moisture. Table 1 contains the different cases. Table 2 refers to the corresponding basic laws, equations and expressions in Table 1. The following chapters will explain the details of these theories and cite some relative examples.

Modes	Inside/surface	Interaction	Objects		
			Heat	Moisture	Coupled heat & moisture
Diffusion	inside	contact	exist (21)	exist (3)	exist (4)
Convection	Surface	contact	exist (22)	exist (5)	exist (7)
Coupled diffusion & convection	Both	contact	exist (24)	exist (6)	exist (8)
Radiation	Surface	remote	exist (23)	No exist	Unknown

Table 1 Physical features of the transport processes
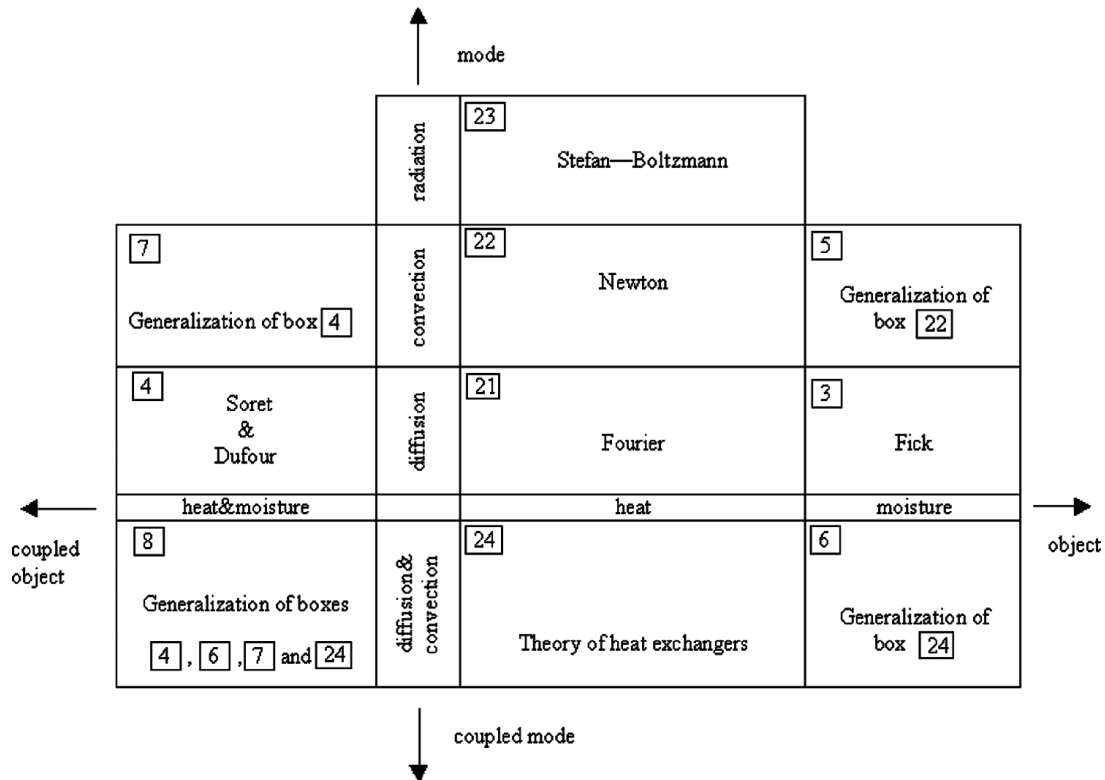
Table 2 Basic Laws and Expressions of the Transport Processes

2.2.2 Heat Transfer

Heat transfer can be characterized by the following three modes and the coupling effects among the three modes.

Heat Conduction

Heat conduction can be expressed by the Fourier's Law:

$$q = -k\,\boldsymbol{\nabla}T \qquad\qquad eq(2.7)$$

where:
$q(x,t) = the\ heat\ flux;$
$T(x,t) = the\ temperature;$
$k \quad = \ the\ coefficient\ of\ heat\ conduction;$
$\boldsymbol{\nabla} \ = \ the\ nabla\ operator;$
$x,t = \ space\ and\ time\ coordinates, respectively$

For convenience of study, the thermal energy concentration *e* is introduced:

$$e = \rho c T \qquad\qquad eq(2.8)$$

where:
$\rho, c \ = the\ mass\ density\ and\ heat\ capacity, respectively$

Normalizing the Fourier's Law:

$$q = -D_T\boldsymbol{\nabla}e;\ D_T = \frac{k}{\rho c} \qquad eq(2.9)$$

where:
$q(x,t) = the\ heat\ flux;$
$D_T \ = \ the\ thermal\ diffusivity;$

Heat Convection

Heat convection can be described by Newton's expression:

$$q = h_T\big(T_s - T_f\big) \qquad\qquad eq(2.10)$$

where:
$q(x,t) = the\ heat\ flux;$
$h_T \ = \ the\ coefficient\ of\ heat\ transfer;$

T_s = the temperatures of the solid boundary;
T_f = the temperature of the fluid boundary;

Heat Radiation

To describe the heat radiation, the Stefan-Boltzmann law is required:

$$W = \varepsilon\, \sigma\, T^4; \qquad\qquad eq(2.11)$$

where:
$W =$ the total power radiated per area per time; $J/(s * m^2)$
$T =$ the absolute temperature; Kelvin
$\varepsilon =$ the emissivity;
$\sigma =$ the Stefan − Boltzmann constant, derives from other known
constants of nature; $(J\, s^{-1} m^{-2} K^{-4})$

Coupled Conduction and Convection of Heat

Figure 4 shows an example of a plane wall with two different temperatures at its two surfaces. Heat conduction takes place in the wall and heat convection occurs at the two surfaces. So, the heat transfer process through the wall is a coupled heat conduction and heat convection process, which can be expressed by the following equation (Szekeres, A. [2012]):

$$q = U(T1 - T2) = \frac{1}{\frac{\delta}{k} + \frac{1}{h_{T1}} + \frac{1}{h_{T2}}}(T1 - T2) \quad eq(2.12)$$

$$U = \frac{1}{R} = \frac{1}{R_1 + R_2 + R_3} \qquad\qquad eq(2.13)$$

where:
$q(x,t) =$ the heat flux;
$\quad U \quad =$ the overall heat transfer coefficient; $\left(\dfrac{W}{m * Kelvin}\right)$
$\quad R \quad =$ the thermal resistance of the barrier; $(\dfrac{m^2 Kelvin}{W})$
$\quad \delta \quad =$ the thickness of the media; (m)
$(T1 - T2) =$ the temperature difference across the media; $(Kelvin)$
$k, h_{T1}\, \&\, h_{T2} =$ thermal conductivity of the media, left & right wall,

$$respectively; (\frac{W}{m * Kelvin})$$
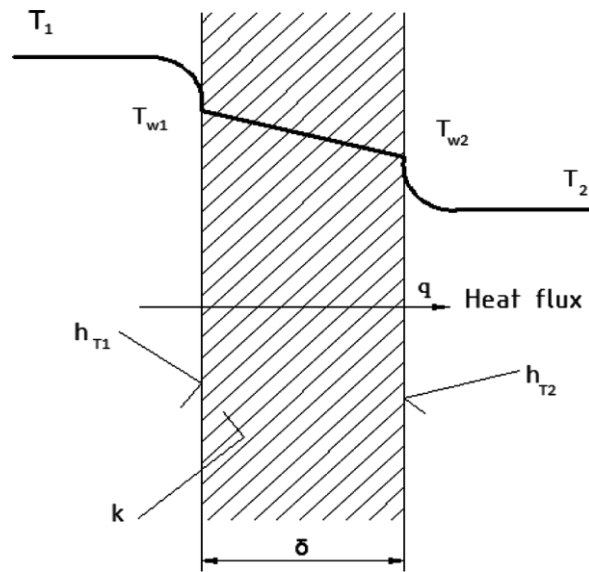
Figure 4 Heat Transfer in a Plane Wall

2.2.3 Moisture Transport

Moisture Diffusion

According to Fick's Law of moisture diffusion, the moisture flux *f* can be calculated as follows:

$$f = -D_m \nabla m ; \qquad\qquad eq(2.14)$$

$where$:
$f(x,t) = the\ moisture\ flux$;
$D_m\quad = the\ mositure\ diffusivity$;
$m\quad = the\ mositure\ concentration$;

In porous materials like concrete, the moisture concentration can be defined as:

$$m = \frac{M}{V} ; \qquad\qquad eq(2.15)$$

where:
$M =$ *the mass of mositure*;
$V =$ *the volume of porous material*;

According to the equation 2.15, the maximum of concentration can be expressed as:

$$m_{max} = \frac{M_{max}}{V} = \frac{V_{voids}\,\rho_{fluid}}{V} = \frac{V_{voids}}{V}\,\rho_{fluid}; \quad eq(2.16)$$

where:
$M_{max} =$ *the maximum mass of moisture*;
$V_{voids} =$ *the total volume of pores*;
$\rho_{fluid} =$ *the density of moisture*;

Based on the results, the moisture-potential (or the normalized moisture concentration) is the following:

$$m^p = \frac{m}{m_{max}} = \frac{M}{V}\frac{1}{\dfrac{V_{voids}}{V}\,\rho_{fluid}} = \frac{M}{V_{voids}\,\rho_{fluid}} \quad eq(2.17)$$

where:
$m^p =$ *the moisture* − *potential*;
$m_{max} =$ *the maximum of concentration*;
Normalizing Fick's law, the moisture flux potential can be described:

$$f = -D_m \boldsymbol{\nabla} m \qquad\qquad eq(2.18)$$

$$\Rightarrow \quad \frac{f}{m_{max}} = -D_m \boldsymbol{\nabla}(\frac{m}{m_{max}}) \qquad\qquad eq(2.19)$$

$$\Rightarrow \quad f^p = -D_m \boldsymbol{\nabla} m^p \qquad\qquad eq(2.20)$$

where:
$\boldsymbol{\nabla} m^p =$ *the gradient of moisture potential*.

Other forms of Fick's law can be formulated depending on the definition of moisture concentration. For example, the moisture concentration can be considered as pore relative humidity, which will be used in the later chapters for the experimental study and thus will be explained in detail.

Moisture Convection

The phenomenon of moisture convection can be characterized by Newton's expression. The moisture flux is the following:

$$f = h_m(m_s - m_l) \qquad eq(2.21)$$

where:
$h_m \quad = the\ coefficient\ of\ moisture\ transfer;$
$m_s\ \&\ m_l = the\ moisture\ concentration\ on\ the\ surface\ of\ the\ porous$
$\qquad material\ and\ in\ the\ bounding\ gas\ or\ liquid, respectively;$

Normalizing by m_{max}, as in the previous section, the moisture flux can be described:

$$f^p = h_m(m_s^p - m_l^p) \qquad eq(2.22)$$

where:
$m_s^p = the\ moisture\ potential\ on\ the\ surface\ of\ the\ solid;$

Note: although the dimensions of the flux potential f^p and of the coefficient of moisture transfer h_m are the same, the two notations should not be confused: f^p is a flux type variable and h_m is a scalar.

Coupled Diffusion and Convection of Moisture

Similar to the situation of coupled heat conduction and heat convection, Figure 5 shows an example of a plane wall with two different moisture concentrations at its two surfaces. Moisture diffusion takes place in the wall and moisture convection occurs at the two surfaces. So, the moisture transport process through the wall is a coupled moisture conduction and moisture convection process, which can be expressed by the following equation (Szekeres, A. [2012]):

$$f = H_m(m_1 - m_2) \qquad eq(2.23)$$

where:

H_m = *the coupling coefficient of moisture transport for the material*; $H_m = \dfrac{1}{\dfrac{\delta}{D_m} + \dfrac{1}{h_{m1}} + \dfrac{1}{h_{m2}}}$

f = *the moisture flux*

m_1 and m_2 = the moisture concentrations on the two side of wall.
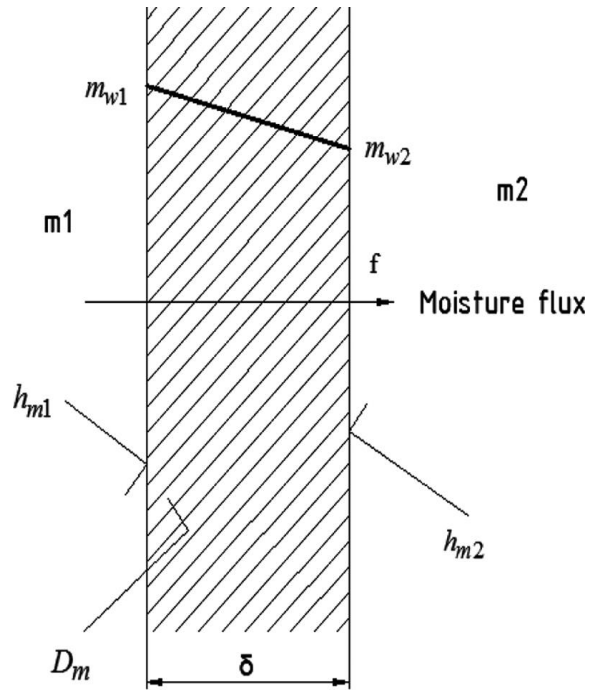
Figure 5 Moisture Transport in Plane Wall

2.2.4 Coupled Heat and Moisture: the Soret and Dufour Effects

Moisture movement in a porous medium can result in heat transfer because moisture can carry heat. This coupling effect is called Dufour effect, and the corresponding heat flux is called the Dufour flux:

$$q = -D_{Tm}\nabla m \qquad eq(2.24)$$

On the other hand, a temperature gradient can drive moisture movement from high temperature side to low temperature side (or from high energy state to low energy state).

The coupling effect is called Soret effect, and the corresponding moisture flux is called the Soret flux:

$$f = -D_{mT}\nabla T \qquad eq(2.25)$$

where:
D_{Tm} & D_{mT} = *the coupled diffusivities* ;
D_{Tm} represents the effect of moisture transport on heat transfer, while D_{mT} represents the effect of heat transfer on moisture transport. In general, $D_{Tm} \neq D_{mT}$.

The general coupled fluxes can be written in the following form when there are more than two driving forces exist:

$$J_i = -D_{ij}\nabla C_j \qquad eq(2.26)$$

where:
i, j = *the summation over the repeated indices* ; $i, j = T, m$

2.2.5 Summary of the Coupling Effects

In summary, the general equations for heat flux and moisture flux can be written as:

$$q = -D_T e_x - D_{Tm} m_x - \boldsymbol{\tau}_T q_t - \boldsymbol{\tau}_{Tm} f_t \qquad eq(2.27)$$

$$f = -D_{mT} e_x - D_m m_x - \boldsymbol{\tau}_{mT} q_t - \boldsymbol{\tau}_m f_t \qquad eq(2.28)$$

where the last two terms on the right hand sides of the two equations represent the effects of heat source (sink) and moisture source (sink) on the two fluxes.

$$\begin{bmatrix} Heat \\ Moisture \end{bmatrix} = \begin{bmatrix} Fourier & Dufour \\ Soret & Fick \end{bmatrix} + \begin{bmatrix} heat & heat/moisture \\ moisture/heat & moisture \end{bmatrix}$$

Figure 6 Basic Law and Expression

The thesis started with the well-known cases formulated by Fourier, Newton, Stefan-Boltzmann, Fick, Soret and Dufour effects. It divided the cases into three major parts: heat transfer, moisture transfer and the coupled effect.

By introducing the notions of heat energy and moisture potential concentrations, the equations and calculations have been simplified and the consistency of the system was made obvious.

2.3 A Case Study

Abstract

A case study will be reviewed as an example for the coupled heat and moisture transfer in concrete (A.Dyan [1981]). A surface heated concrete slab has been studied to learn the relationship between heat and mass transfer in the concrete. Concrete is treated as a porous material containing water, vapor and air. The solution is an explicit numerical scheme. The results are the temperature, pore pressure and moisture distributions as functions of time. The results demonstrate the relationship between moisture and heat transfer.

Introduction

Heating concrete on the surface may cause the evaporation of water when the temperature is well above boiling temperature of water. The pore pressure generated by the steam weakens the concrete and may cause cracking and spalling damage when the pressure is high. This phenomenon is very complicated since it involves coupled heat and moisture transfer as well as phase transformation. Evaluation of concrete at elevated temperatures is important for safety assessments of concrete structures.

Heating concrete causes the evaporation of water and the subsequent pressurization of both vapor and air within the pores. The migration of vapor and air that follows the pressurization results in the release of vapor from the structure's boundaries. Sustained heating leads to continuous evaporation and drying of the region near the surface. In the deeper region where the concrete is still cold, the concrete remains wet and actually gains moisture from recondensation.

The evaporation-recondensation mechanism was found to play an important role in the behavior of concrete under elevated temperatures. An evaporation-recondensation model was applied to two separate solutions to study the behavior of concrete. One is the implicit numerical scheme, where the lower order terms were neglected and material properties were assumed constants. The other one is the explicit numerical scheme which solves the governing equations, taking into account the terms for liquid moisture filtration and moisture dependent material properties.

The purposes of this case study are to develop the numerical model and compare the model prediction with the experimental data.

Mathematical Model

The specimen is a concrete slab consisting of hydrated cement paste with no aggregates. Following intense heating of the concrete surface, the region near the surface dries out. Evaporation takes place exclusively at the interface between the dry and the wet regions. The transport of gas occurs under pressure and concentration gradients. The migration of liquids is primarily governed by pressure gradients. Under sustained surface heating, the dry zone expands into the concrete.
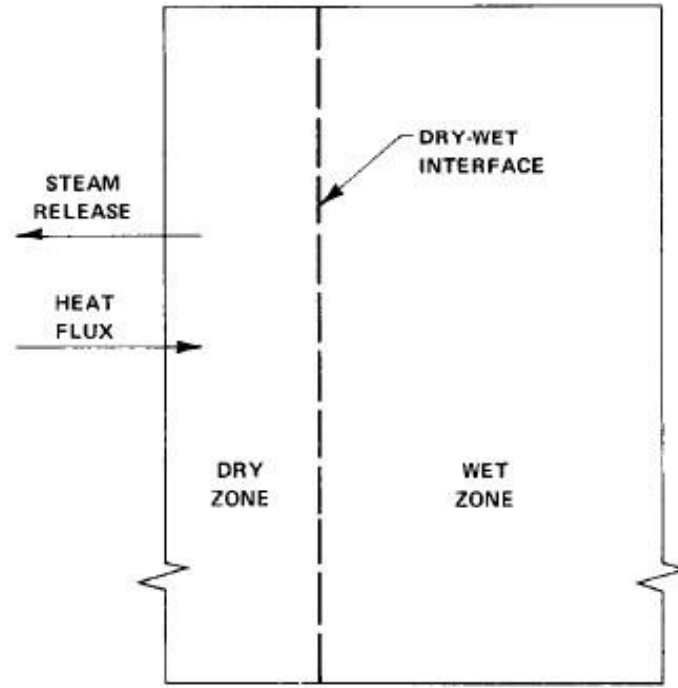
Figure 7 Physical Model of a Heated Concrete Slab (A.Dyan [1981])

The conservation equation for mass and energy in the dry zone are written as:

$$\varepsilon\frac{\partial\rho_i}{\partial t} + \frac{\partial}{\partial x}\left(u_g\rho_i + j_i\right) = 0 \quad i = 2,3 \qquad (eq\ 2.29)$$

$$(1-\varepsilon)\rho_0\frac{\partial e_0}{\partial t} + \sum_{i=2}^{3}\left[\varepsilon\frac{\partial(\rho_i e_i)}{\partial t} + \frac{\partial}{\partial x}\left(u_g\rho_i + j_i\right)h_i\right] = K_d\frac{\partial^2 T}{\partial x^2} \quad (eq\ 2.30)$$

where:
$\varepsilon \ = \ $ *the porosity*;
ρ_2 & $\rho_3 \ = \ $ *the density of vapor and air*;
$t \ = \ $ *the time*;
$u_g \ = \ $ *the volumetric flow rate of gases in the x direction per unit area*;
j_2 & $j_3 \ = \ $ *the diffusive mass flux of vapor and air*;
$e \ = \ $ *the specific internal energy*;
$h \ = \ $ *the specific enthalpy*;
$K_d \ = \ $ *the thermal conductivity of the dry zone*;
$T \ = \ $ *the temperature in ^oC*;

The conservation equation for mass and energy in the wet zone are written as:

$$\varepsilon\frac{\partial}{\partial t}[(1-S)\rho_1 + S\rho_2] + \frac{\partial}{\partial x}\left(u_1\rho_1 + u_g\rho_2 + j_2\right) = 0 \qquad (eq\ 2.31)$$

$$\varepsilon \frac{\partial}{\partial t}(S\rho_3) + \frac{\partial}{\partial x}(u_g\rho_3 + j_3) = 0 \qquad\qquad (eq\ 2.32)$$

$$(1-\varepsilon)\rho_0 \frac{\partial e_0}{\partial t} + \varepsilon \frac{\partial}{\partial t}[(1-S)\rho_1 e_1 + S(\rho_2 e_2 + \rho_3 e_3)] +$$

$$\frac{\partial}{\partial x}[u_1\rho_1 h_1 + (u_g\rho_2 + j_2)h_2 + (u_g\rho_3 + j_3)h_3] = K_w \frac{\partial^2 T}{\partial x^2} \qquad (eq\ 2.33)$$

where:
S = *the volume fraction of the pores occupied by gases*;
ρ_1 = *the density of liquid*;
u_1 = *the liquid apparent velocity*;
e_1 & h_1 = *the liquid specific energy and enthalpy, respectively*;

The following equations are the relating coefficients. The filtration velocity of gas

phase is found according to Darcy's law:

$$u = -\frac{k(S)}{\mu}\frac{\partial P}{\partial x} \qquad\qquad (eq\ 2.34)$$

where:
u = *the filtration velocity of gas phase*;
P = *the pore pressure*;
μ = *the viscosity*;
$k(S)$ = *the permeability; it is assumed to be directly proportional to gas*
 volume fraction within the pores: $k(S) = k_d S$
 (k_d = *the permeability of dry concrete*)

The diffusive flux of the ith gaseous species is according to Fick's law:

$$j_i = -\rho D(S)\frac{\partial w_i}{\partial x} \qquad\qquad (eq\ 2.35)$$

where:
ρ = *the air – vapor mixture density* ;
w_i = *the mass fraction of the ith species* ;
$D(S)$ = *the moisture dependent coefficient*; $D(S) = D_d S$ (D_d *is the diffusion*
 coefficient of dry concrete)

Air and water vapor are similarly considered as an ideal binary mixture and according

to Dalton's law:

$$P_i = \rho_i R_i T_a \qquad\qquad (eq\ 2.36)$$

$$e_i = c_i T \qquad\qquad (eq\ 2.37)$$

$$h_i = c_{pi} T \qquad\qquad (eq\ 2.38)$$

$where$:
$R_i = the\ gas\ constant\ of\ the\ ith\ species$;
$T_a = the\ absolute\ temperature$; $(Kelvin)$
$c\ \&\ c_a = the\ specific\ heat\ at\ constant\ volume\ and\ at\ constant\ pressure, respectively$;

Solution Method

An explicit numerical scheme was used to solve the governing equations depending on the initial and boundary conditions. The slab was subdivided into a finite number of equally spaced nodal points. The dry-wet interface was assumed to be located right in between the dry and wet nodal points. When local dry out is reached, the dry-wet interface relocates to separate the next two nodes. Because pressure depends on local temperature, the sudden jumps of the interface produce fluctuations in pressure which can be reduced by decreasing the grid size.

In the dry region, the governing equation is represented as a form readily suitable for explicit representation of density and temperature variations with time. The divergence terms of the equation give the density time derivatives. And the derivatives and divergence terms of the equation give the temperature time derivative. Then the new property distributions should be calculated based on known distributions at a previous time step.

The wet region gets an additional variable when compared to the dry region. The variable is the volume fraction of the pores occupied by vapor. Calculating the time derivative of S first is necessary in order to proceed with the computation of all other

parameters for the dry region with the same routine. Knowing the value of S also ensures the location of the dry-wet interface.

In order to calculate the value of S the following definitions are made:

$$V_1 = \frac{\partial}{\partial x}(u_1\rho_1 + u_g\rho_2 + j_2) \qquad (eq\ 2.39)$$

$$V_2 = \frac{\partial}{\partial x}(u_g\rho_3 + j_3) \qquad (eq\ 2.40)$$

$$V_3 = \frac{\partial}{\partial x}\left[u_1\rho_1 h_1 + (u_g\rho_2 + j_2)h_2 + (u_g\rho_3 + j_3)h_3 - K_w\frac{\partial T}{\partial x}\right] \qquad (eq\ 2.41)$$

$$V_4 = c_2 T + \left[\begin{matrix}(1-\varepsilon)\rho_0 c_0 + \varepsilon\rho_1 c_1(1-S)\\ +\varepsilon S(\rho_2 c_2 + \rho_3 c_3)\end{matrix}\right] / (\varepsilon S\frac{\partial \rho_2}{\partial T}) \qquad (eq\ 2.42)$$

Note: the first three show divergences of flux. The square brackets in the fourth one show the volumetric heat capacity of the concrete and its constituents.

The vapor density temperature derivative can be obtained from the saturation density-temperature derivative:

$$\rho_2 = 1.055 \times 10^{21} T_a^{-6} R_2^{-1} exp\left(-\frac{7000}{T_a}\right) \qquad (eq\ 2.43)$$

Note: according to the Clausius-Clapeyron equation, the temperature-pressure should be:

$$P = 1.055 \times 10^{21} T_a^{-5} exp\left(-\frac{7000}{T_a}\right) \qquad (eq\ 2.44)$$

$$\frac{\partial \rho_2}{\partial t} = \frac{\partial \rho_2}{\partial T}\frac{\partial T}{\partial t} \qquad (eq\ 2.45)$$

The temperature time derivatives in equation 2.33 are converted to vapor density derivatives by introducing equations 2.44 and 2.45. And then the densities time

derivatives from equations (3) and (4) are substituted in equation (5) to get the time derivative of S:

$$\frac{\partial S}{\partial t} = \frac{1}{\varepsilon} \left[\frac{V_1 V_4 + c_3 T V_2 - V_3}{V_4 (\rho_1 - \rho_2) + \rho_1 u_{fg} + (\rho_2 c_2 - \rho_1 c_1) T} \right] \qquad (eq\ 2.46)$$

For the stability of the numerical calculations, there needs to be three stability criteria for time step:

$$The\ heat\ conduction: \Delta t \leq \frac{(1 - \varepsilon) \rho_0 c_0 \Delta x^2}{2 K_w} \qquad (eq\ 2.47)$$

$$The\ mass\ diffusion\ mechanism: \Delta t \leq \frac{\varepsilon \Delta x^2}{2D} \qquad (eq\ 2.48)$$

$$The\ filtration\ mechanism: \Delta t \leq \frac{\varepsilon \mu}{2k} \frac{\Delta x^2}{P_{max}} \qquad (eq\ 2.49)$$

$where$:
$\Delta t = the\ time\ incremental$;
$\Delta x = the\ grid\ size$;
$c_0 = the\ specific\ heat\ of\ solid\ structure$;

Results and Conclusions

The simulation (A.Dyan [1981]) was a cylindrical concrete slab, 0.6 m diameter and 0.3 m thick. It was heated by a steel plate on one side and maintained at room temperature on the other side. Temperature and pressure were recorded at different axial locations. Vapor released from the concrete was collected and weighted at various times.

Symbol	Value	Dimensions
ρ_0	2500	$kg\,m^{-3}$
ρ_1	1000	$kg\,m^{-3}$
c_0	1000	$J\,kg^{-1}\,^{\circ}C^{-1}$
c_{p1}	4200	$J\,kg^{-1}\,^{\circ}C^{-1}$
c_{p2}	2016	$J\,kg^{-1}\,^{\circ}C^{-1}$
c_{p3}	1050	$J\,kg^{-1}\,^{\circ}C^{-1}$
ε	0.32	None
K_d	0.35	$W\,m^{-1}\,^{\circ}C^{-1}$
K_w	1.6	$W\,m^{-1}\,^{\circ}C^{-1}$
k/μ	2.4×10^{-6}	$m^2\,atm^{-1}\,s^{-1}$
$(k/\mu)_{liquid}$	2.4×10^{-10}	$m^2\,atm^{-1}\,s^{-1}$
D_d	10^{-6}	$m^2\,s^{-1}$

Table 3 Material Properties used in the Test Analysis

In this simulation, the concrete contained a magnetite aggregate, the water to cement ratio was 0.5 and the specimen was 47 days old. Atmospheric pressure of dry air was assumed to exist near the specimen's surface. The locations of record were 2.56, 7.62 and 12.7 cm from the heated surface.
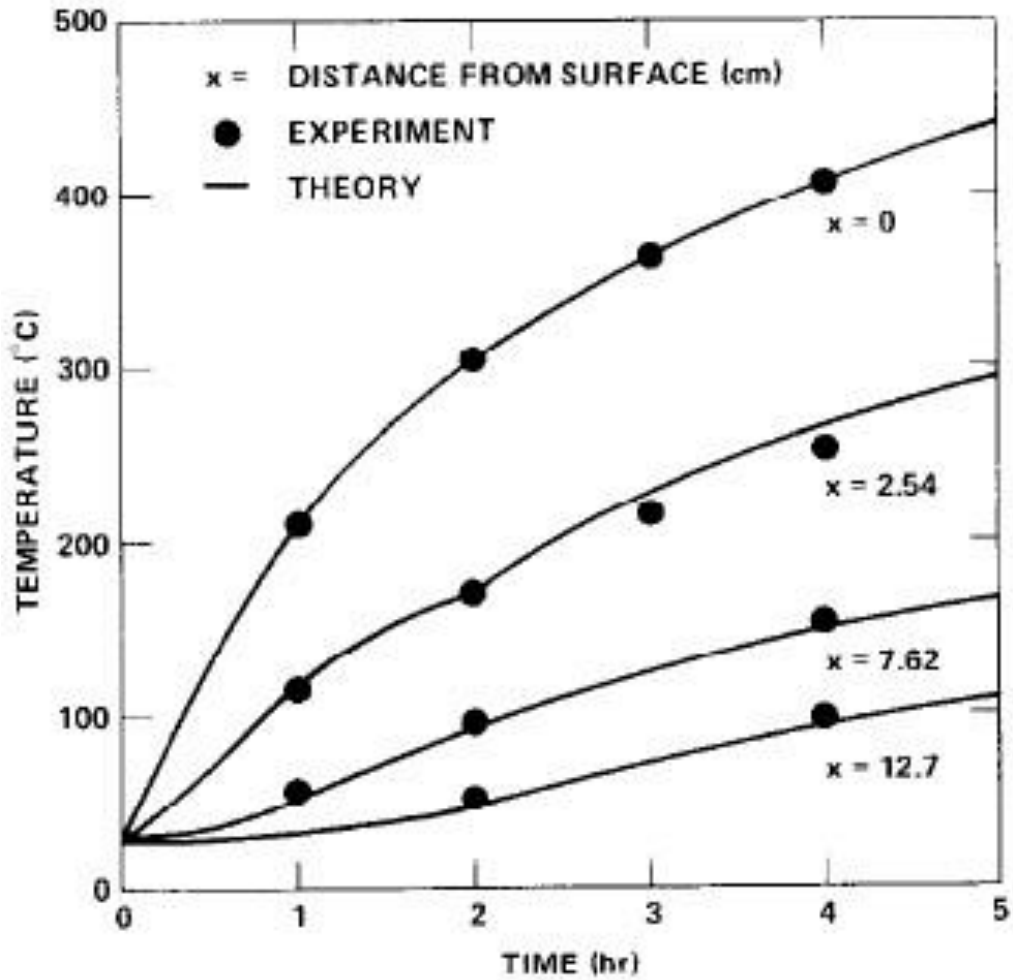
Figure 8 Thermal Response of a Heated Concrete Slab (A.Dyan [1981])

The temperature increases while the distance from the surface decreases. Furthermore, the figure shows that the inside temperature of the slab is around 100 ^{o}C, which is very high.
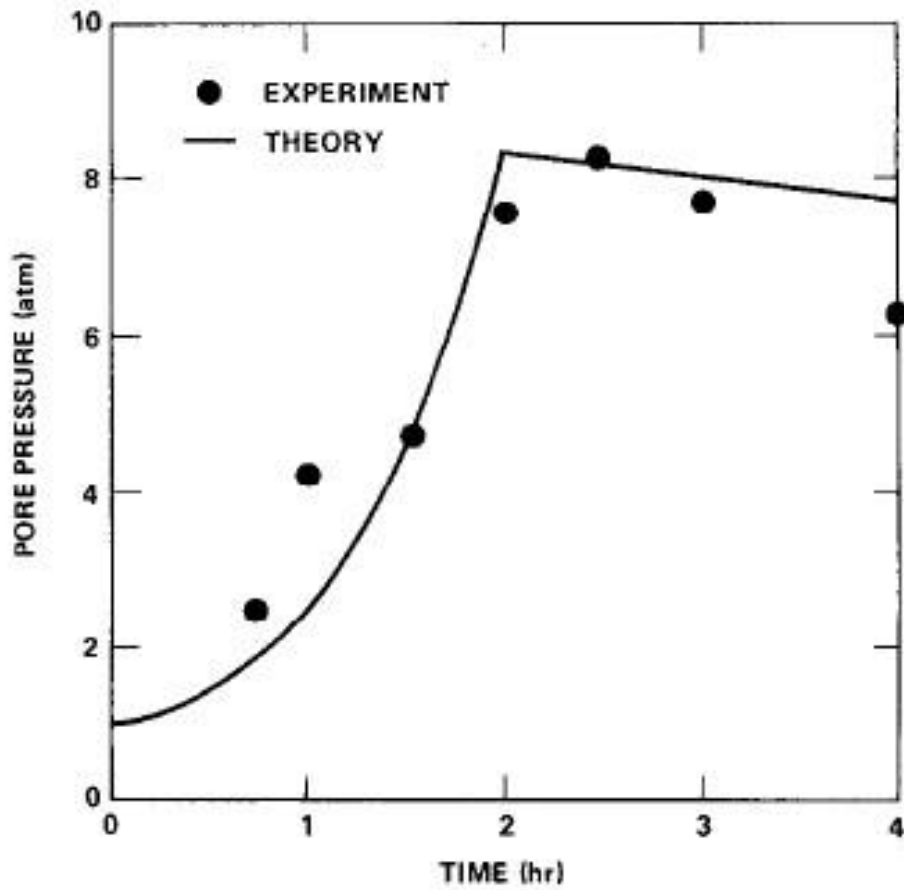
Figure 9 Pressure Responses at Depth of 2.54 cm (A.Dyan [1981])

The sudden change in the rate of temperature at 2 hours, at a depth of 2.54 cm, can indicate that the dry-wet interface occurred. Additionally, the pressure response also reaches the peak value.
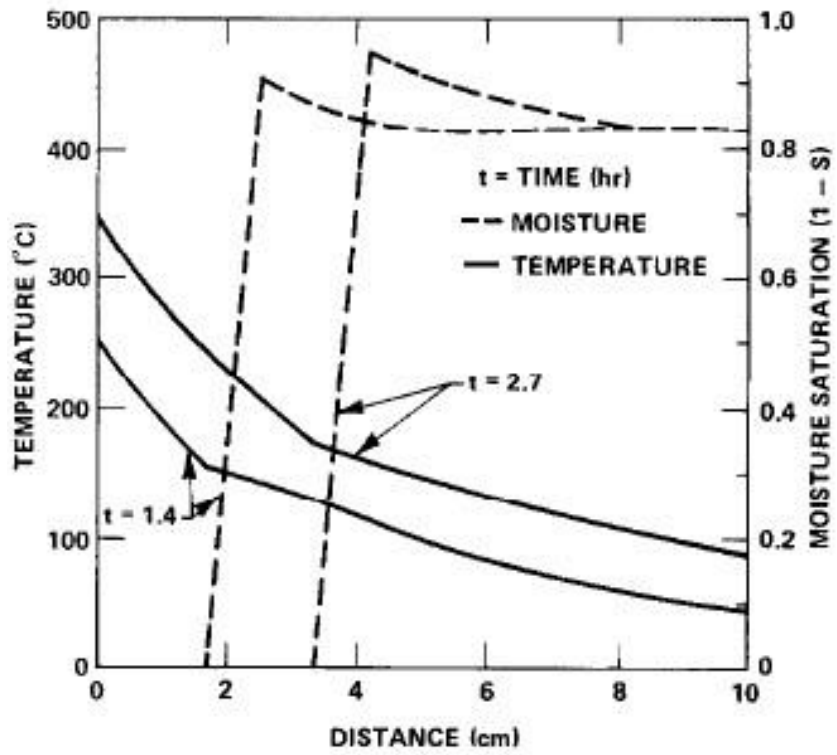
Figure 10 Distributions of Temperature and Moisture (A.Dyan [1981])
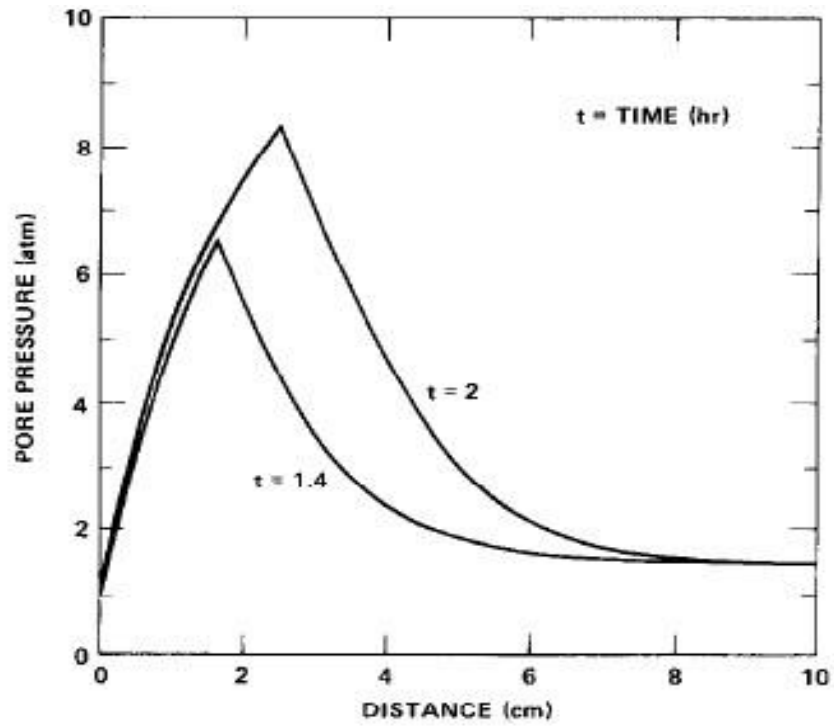
Figure 11 Pore Pressure Distributions (A.Dyan [1981])

The turning point of temperature in Fig.10 (A.Dyan [1981]) represents the location of the dry-wet interface. The reduced temperature gradient is produced by the enhanced heat transfer resulting from a higher thermal conductivity and the evaporation-recondensation mechanism. The moisture distribution shows a high value near the interface.

Fig.11 (A.Dyan [1981]) shows that the peak pore pressure exists near the interface. Therefore, if the peak value was sufficient to create cracking, one would expect to find wet fracture surfaces.

In conclusion, concrete interactions with hot metals can result in concrete spallation and exposure of totally wet fracture surfaces. In order to obtain a more exact shape, one must know the exact position of the dry-wet interface.

CHAPTER 3

GOVERNING EQUATIONS FOR THE COUPLED TEMPERATURE AND MOISTURE TRANSPORT IN CONCRETE

3.1 Introduction

Moisture content is of considerable concern for predicting the serviceability and durability of cementitous materials. Moisture distribution within concrete structures is important for evaluating the time-dependent phenomena such as creep, shrinkage, fire resistance, and other long-term durability properties of concrete.

As discussed in earlier chapters, to predict moisture transfer in concrete, one should not only study the effect of moisture gradient, but also consider the effect of temperature gradient, i.e. the Soret effect. This chapter will present some governing equations for the coupled moisture transport which will be used in the next chapter to determine the coupling parameters based on the experimental results.

3.2 Moisture and Heat Fluxes

Under non-saturated and non-isothermal condition, the flux of moisture in concrete includes the flux due to the gradient of moisture concentration according to Fick's first law as well as the flux due to the gradient of temperature described by, the Soret effect. Similarly, the heat flux should consist of the flux due to the temperature gradient governed by the Fourier law, and the flux due to the gradient of moisture concentration descried by the Dufour effect.

Accordingly

$$J = -D_{HH} \, grad \, H - D_{HT} \, grad \, T \qquad (eq \ 3.1)$$

$$q = -D_{TH} \, grad \, H - D_{TT} \, grad \, T \qquad (eq \ 3.2)$$

$where$:
$J \ = \ the \ flux \ of \ moisture \ in \ concrete; \ unit: kg/m^3$
$q \ = \ the \ flux \ of \ heat \ in \ concrete; \ unit: K/m^3$
$H \ = \ the \ pore \ relative \ humidity \ in \ concrete;$
$T \ = \ the \ temperature;$
$D_{HH} \ and \ D_{TT} = the \ coefficients \ of \ diffusion \ ;$
$D_{HT} \ and \ D_{TH} \ = the \ two \ coupling \ parameters;$

It is important to note that in the present study the moisture gradient in concrete is expressed in terms of pore relative humidity, H, in the above governing equations. This is because the moisture in the pores of concrete is a mixture of liquid water, vapor, and dry air. The moisture in most of concrete structures such as bridges, pavement, and buildings does not exist in liquid phase and is not even in a saturated stage. Therefore, using the gradient of water pressure as a driving force (as in Darcy's law) is not valid for most of practical cases. On the other hand, the water in concrete has several different forms. For example, chemically combined water is the water consumed during the hydration reactions between Portland cement and water; the water in gel pores (nanometer size pores) is confined and thus not mobile (not available for diffusion). Furthermore, the amounts of chemically combined water and the gel water are functions of time depending on the degree of hydration and the evolution of cement paste microstructure. Therefore, using the gradient of moisture content in concrete will make the governing equations very complicated. As an alternative, the pore relative humidity, H, has been used as a basic variable and the gradient of H as a driving force. H is the relative pressure generated by

the mixture of water, vapor, and dry air in pores, which does not include the chemically

combined water and etc.

$$H = -P/P_S \qquad (eq\ 3.3)$$

where:
H = *relative pressure*;

P = *pore pressure*;

P_S = *saturated pore pressure*;

3.3 Derivation of the Balance Equation

Temperature

The balance equation:

$$\frac{\partial Q}{\partial t} = -\nabla . q + S_Q \qquad (eq\ 3.4)$$

where:
$Q = heat$;
$q = temperature\ flux$;
$S_Q = heat\ source\ or\ sink;\ simily, set\ S_Q = 0$;

$$q = -D_{TH}\ grad\ H - D_{TT}\ grad\ T \qquad (eq\ 3.5)$$

After combining the above two equations together, the balance equation can be

described as:

$$\frac{\partial Q}{\partial t} = -\nabla . (-D_{TH}\ grad\ H - D_{TT}\ grad\ T) \qquad (eq\ 3.6)$$

Since heat Q is a function of T, the left hand side of the equation can be further

manipulated as

$$\frac{\partial Q}{\partial T}\frac{\partial T}{\partial t} = \nabla . (D_{TH}\ grad\ H + D_{TT}\ grad\ T) \qquad (eq\ 3.7)$$

where $\partial Q/\partial T$ = heat capacity (or specific heat), which is a material property. Now, this basic equation is expressed in terms of two variables, T and H.

Moisture

The conservation of the mass equation is described as:

$$\frac{\partial w}{\partial t} = -\nabla.J + S_w \qquad (eq\ 3.8)$$

where:
w = *moisture content in concrete*;
J = *moisture flux*;
S_w = *moisture source or sink*;

Note: S_w is not significant and can be taken as zero for most of existing structure under ambient temperature. However, it is important for some special cases. For example, under high temperatures, it is required to account for the water released by dehydration due to heating. Consequently, the mass balance equation can be simplified:

$$\frac{\partial w}{\partial t} = -\nabla \cdot J \qquad (eq\ 3.9)$$

$$J = -D_{HH}\ grad\ H - D_{HT}\ grad\ T \qquad (eq\ 3.10)$$

Combining the two equations, the mass balance equation can be described as:

$$\frac{\partial w}{\partial t} = -\nabla \cdot (-D_{HH}\ grad\ H - D_{HT}\ grad\ T) \qquad (eq\ 3.11)$$

Since moisture content is a function of H, the left hand side of the equation can be further manipulated as

$$\frac{\partial w}{\partial H}\frac{\partial H}{\partial t} = \nabla \cdot (D_{HH}\ grad\ H + D_{HT}\ grad\ T) \qquad (eq\ 3.12)$$

where $\partial w/\partial H$ = moisture capacity, which is a material property. Now, this basic equation, similar to the equation for the heat, is also expressed in terms of two variables, T and H.

Summary

The balance equations for heat and moisture are, respectively:

$$\frac{\partial Q}{\partial T}\frac{\partial T}{\partial t} = \nabla \cdot (D_{TH} \ grad \ H + D_{TT} \ grad \ T) \qquad (eq \ 3.13)$$

where:

$$\frac{\partial Q}{\partial T} = the \ heat \ capacity \ ;$$

$$D_{TT} = the \ thermal \ diffusion \ coefficient;$$

$$D_{TH} = the \ coupling \ parameter \ for \ Dufour \ effect;$$

$$\frac{\partial w}{\partial H}\frac{\partial H}{\partial t} = \nabla \cdot (D_{HH} \ grad \ H + D_{HT} \ grad \ T) \qquad (eq \ 3.14)$$

where:

$$\frac{\partial w}{\partial H} = the \ moisture \ capacity \ ;$$

$$D_{HH} = the \ moisture \ diffusion \ coefficient;$$

$$D_{HT} = the \ coupling \ parameter \ for \ Soret \ effect;$$

$$Note: generally \ D_{TH} \neq D_{HT}$$

The two variables T and H can be solved by the two equations with properly defined initial and boundary conditions. As one can see, there are six material parameters in the two equations: two capacities, two diffusion coefficients, and two coupling parameters. There have been many researches on the two capacities and two diffusion coefficients, which will not be repeated in the present study. The next chapter will focus on one of the coupling parameters, D_{HT}, which is the effect of temperature on moisture transfer. An

experimental study will be carried out, and the coupling parameter will be determined by using the test data.

CHAPTER 4

AN EXPERIMENTAL STUDY ON THE COUPLING PARAMETER

4.1 Experimental Design

The objective of this chapter is to determine the temperature effect on the moisture transport in concrete. In order to understand the coupling phenomenon, temperature gradient was considered as the only influential parameter in the experimental study. The experimental setup is shown in Fig. 12. Two cylindrical specimens are subjected to two moisture transport processes from the top surface.   The bottom surfaces of the two specimens are exposed to the same ambient conditions of the lab, the same ambient temperature and relative humidity. The side wall of the concrete cylinders was sealed to prevent any moisture exchange and insulated to prevent the heat loss. In Fig. 12, the moisture transport in the concrete cylinder on the left is driven by the moisture gradient only, and there is no temperature gradient in the specimen. The moisture transport in the concrete cylinder on the right is driven by both the moisture gradient and temperature gradient. So, if there is any difference in the measured moisture concentration profiles in the two specimens, the difference must be caused by the temperature gradient. In this way, the effect of temperature on the moisture transport can be characterized, and the test data can be used to determine the coupling parameter, $D_{HT,}$ representing the effect of temperature on moisture transport.

In order to determine if the coupling parameter is temperature dependent or not, three different water temperatures were used: 70 ^{o}C, 40 ^{o}C and room temperature. Comparing the two concentration profiles of the specimens under room temperature and 40 ^{o}C, one

coupling parameter D_{HT} can be obtained. Then, comparing the two concentration profiles of the specimens under room temperature and 70 $^{\circ}$C, another coupling parameter D_{HT} can be obtained. If the two coupling parameters are about the same, the coupling parameter is not temperature dependent. Otherwise, it is temperature dependent.
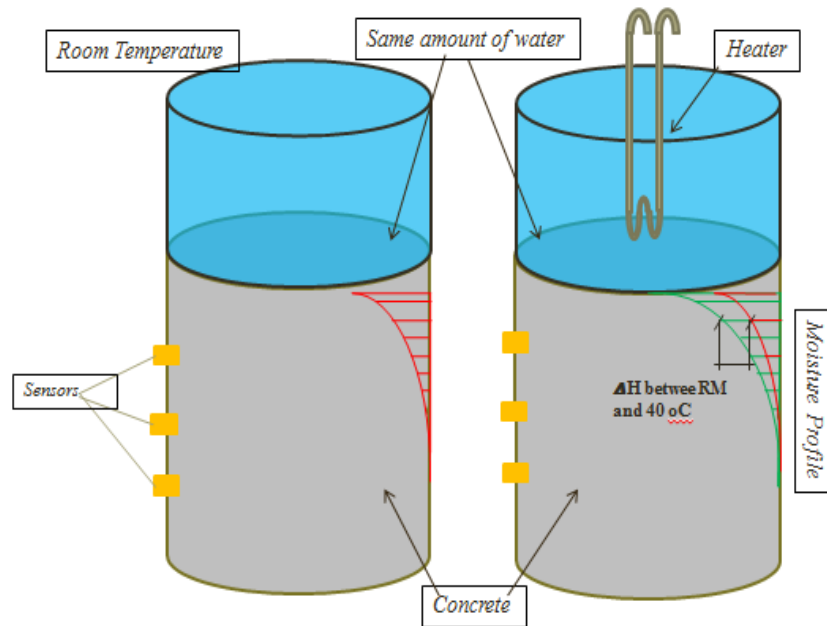
Figure 12 the Model for the Experimental Topic

In order to exclude the effect of other parameters, the three specimens were cast using the same concrete mix design, the same materials, at the same time and cured for the same period. Throughout the experimental period, the specimens were under the same water pressure (the water levels in the top ponds were kept the same). In general, the only experimental variable was the water temperature on the top surface of concrete cylinders.

4.2 Experimental Procedure

The mold for the specimen was plastic cylinder of 6"×12" (diameter × height). The cement was Type I Portland cement. The average size of the aggregate was 0.5". Fine

aggregate was all-purpose sand from Home Depot. Table 4 shows the concrete mix design.

w/c=0.6; s/c=2.4; g/c=2.9; loss factor=1.1		
Component	Mass (g)	Consider the loss factor (g)
cement	2278	2505
water	1367	1503
sand	5466	6013
aggregate	6605	7265

Table 4 The Concrete Mix Design

After 28 days of curing in the cure room, the specimens were moved out of the curing room and kept in the room environment to make the inside of the specimens the same temperature and moisture condition with the surrounding environment.

The sensors used in this experiment were SHT75 Sensirion humidity and temperature sensors, as show in Figure 13. This sensor measures the internal relative humidity and temperature in the pores.

Figure 13 the SHT75 Sensor

Each sensor was plugged into a plastic tube. Both end sides of the tube were wrapped by GoreTex and sealed with epoxy. Then the assemblies were embedded into holes which were drilled into the side of the concrete cylinder. The locations were 2.5", 5.5" and 8.5" from the top surface.

After installing the sensors, the side of the cylinder was covered with silicone and insulated by cotton to ensure that moisture and temperature can only penetrated the specimen in one direction from the top surface. The 6 inch tall plastic sleeves were produced from the molds. This could create a 4 inch deep reservoir on top of each specimen. Each sleeve was clamped to the specimen with a standard steel band clamp. A bead of silicone was added to the inside of each sleeve to further prevent water leakage. The result was a water tight reservoir on top of each specimen. Furthermore, the top of the reservoir was covered in foil to decrease the loss rate of water due to evaporation. The assembly is shown in Figure 14.
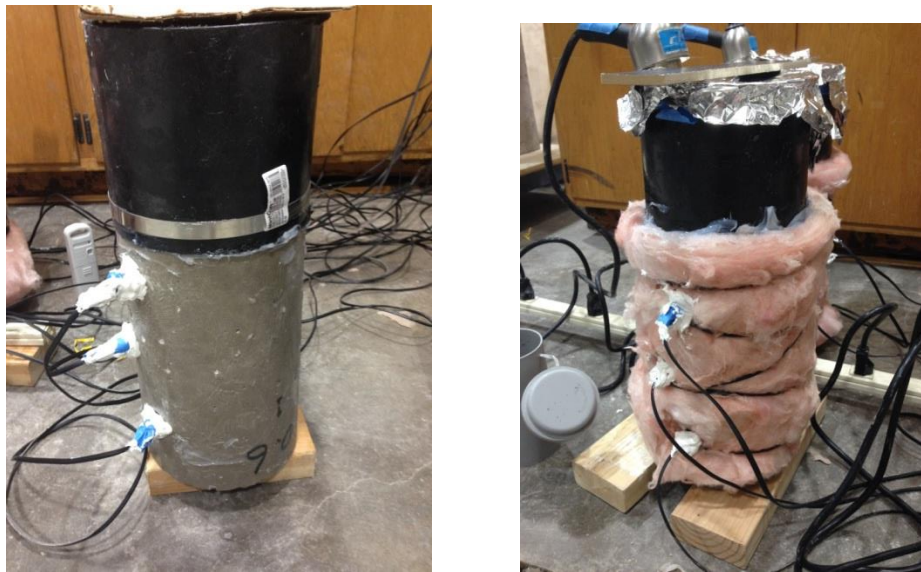
Figure 14 the Specimen Ready for Testing

The experiment used Cole-Parmer electric heaters (model EW-03046-20) with dial temperature controllers. A figure for the heater is shown in Figure 15.

Figure 15 Cole-Parmer EW-03046-20 Electric Heater

The data from the sensors was recorded using an EK-H3 Sensirion Data Logger. Data was recorded every minute.

Three concrete cylinders for the compression test were 3"×6". The test was performed after 28 curing days. The compressive strength of the first, second and third specimens were 3.94 ksi, 3.51 ksi, 3.53 ksi, respectively. Details are listed in Appendix A.

4.3 Experimental Results

The concrete samples were cast and cured for 28 days, from 1/24/2014 to 2/21/2014; after fully curing, they were left in the lab environment for 20 days until 3/13/2014 and then the experiment started. After 15 days, on 3/27/2014, two damaged sensors were replaced. The records which were discussed in the following began on 3/28/2014.

For room temperature case, the moisture value under different time and location					
Time	15 day (3/28/2014)			17 day		
x (in)	2.5	5.5	8.5	2.5	5.5	8.5
x (mm)	63.5	139.7	215.9	63.5	139.7	215.9
H (%)	59.39	38.98	32.83	60.41	39.97	33.89
Time	19 day			21day		
x (in)	2.5	5.5	8.5	2.5	5.5	8.5
x (mm)	63.5	139.7	215.9	63.5	139.7	215.9
H (%)	61.76	41.11	34.94	61.76	41.11	34.94

Table 5 the Moisture for Room Temperature Case

For room temperature, the temperature value under different time ;				
Time	15 day	17 day	19 day	21 day
T (^{o}C)	24.1	24.23	24.2	24
T (K)	297.25	297.38	297.35	297.15

Note: the inside temperature for different locations is almost constant;

Table 6 the Temperature for Room Temperature Case

For 40 ^{o}C case, the moisture value under different time and location					
Time	15 day			17 day		
x (in)	2.5	5.5	8.5	2.5	5.5	8.5
x (mm)	63.5	139.7	215.9	63.5	139.7	215.9
H (%)	63.04	44.23	38.4	64.27	45.49	39.36
Time	19 day			21 day		
x (in)	2.5	5.5	8.5	2.5	5.5	8.5
x (mm)	63.5	139.7	215.9	63.5	139.7	215.9
H (%)	65.67	46.88	40.76	67.11	48.32	42.2

Table 7 the Moisture for 40 ^{o}C Case

For 40 °C case, the temperature value under different time and location					
Time	15 day			17 day		
x (in)	2.5	5.5	8.5	2.5	5.5	8.5
x(mm)	63.5	139.7	215.9	63.5	139.7	215.9
T (°C)	29.55	28.36	27.29	29.96	28.77	27.71
Time	19 day			21 day		
x (in)	2.5	5.5	8.5	2.5	5.5	8.5
x(mm)	63.5	139.7	215.9	63.5	139.7	215.9
T (°C)	30.43	29.25	28.2	31	29.81	28.77

Table 8 the Temperature for 40 °C Case

For 70 °C case, the moisture value under different time and location					
Time	15 day			17 day		
x (in)	2.5	5.5	8.5	2.5	5.5	8.5
x (mm)	63.5	139.7	215.9	63.5	139.7	215.9
H (%)	79.85	51.63	43.59	81.4	53.17	45.13
Time	19 day			21 day		
x (in)	2.5	5.5	8.5	2.5	5.5	8.5
x (mm)	63.5	139.7	215.9	63.5	139.7	215.9
H (%)	83	54.77	46.72	84.6	56.36	48.31

Table 9 the Moisture for 70 °C Case

For 70 °C case, the temperature value under different time and location					
Time	15 day			17 day		
x (in)	2.5	5.5	8.5	2.5	5.5	8.5
x(mm)	63.5	139.7	215.9	63.5	139.7	215.9
T (°C)	43.74	42.5	41.7	45.03	43.61	42.74
Time	19 day			21 day		
x (in)	2.5	5.5	8.5	2.5	5.5	8.5
x(mm)	63.5	139.7	215.9	63.5	139.7	215.9
T (°C)	46.17	44.95	44.04	47.2	45.99	45.12

Table 10 the Temperature for 70 °C Case

4.4 Analysis of The Experimental Results

Using the test data, the trend lines were obtained which show the moisture and temperature at different depths in the sample:
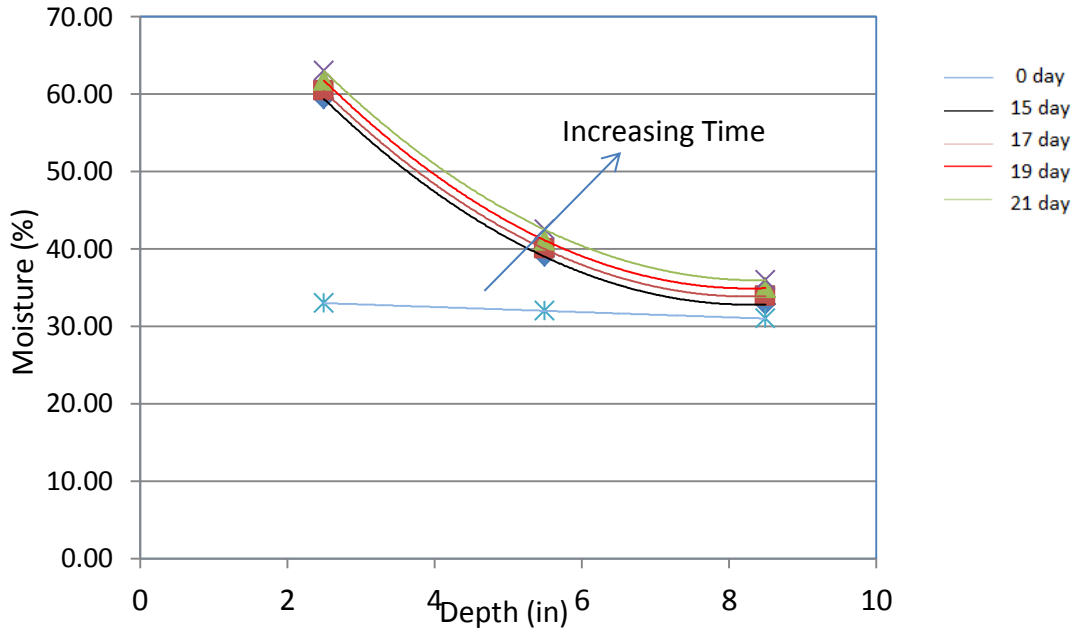
Figure 16 Depths vs. Moisture for Room Temperature Case

The above figure shows the moisture profiles under room temperature at different times. In Figure 16, the initial moisture which is before adding the water tight reservoir is almost constant through the sample. After 15 days, the moisture distribution is higher in the left side, which is near the ponding surface. As time increases, the left side almost keeps constant which means the side may reach the maximum value. However, the right side increases with time increasing.

Depending on the records from the three sensors at 2.5", 5.5" and 8.5", they can provide a 2 order polynomial equation to represent the trend line and calculate the value of humidity at other locations. The final results are shown in the following tables:

Time	15 day						
x (in)	2.5	3	3.5	4	4.5	5	5.5
x (mm)	63.5	76.2	88.9	101.6	114.3	127	139.7
H (%)	59.39	55.00	51.00	47.40	44.20	41.39	38.98
Time	17 day						
x (in)	2.5	3	3.5	4	4.5	5	5.5
x (mm)	63.5	76.2	88.9	101.6	114.3	127	139.7
H (%)	60.41	56.01	52.00	48.39	45.19	42.38	39.97
Time	19 day						
x (in)	2.5	3	3.5	4	4.5	5	5.5
x (mm)	63.5	76.2	88.9	101.6	114.3	127	139.7
H (%)	61.76	57.31	53.27	49.62	46.38	43.54	41.11
Time	21 day						
x (in)	2.5	3	3.5	4	4.5	5	5.5
x (mm)	63.5	76.2	88.9	101.6	114.3	127	139.7
H (%)	63.01	58.61	54.60	50.99	47.76	44.92	42.47

Table 11 the Moisture for Room Temperature

Test day	15	17	19	21
T (^{o}C)	24.1	24.23	24.2	24
T (K)	297.25	297.38	297.35	297.15
Note: due to no temperature gradient, the inside temperature is almost same.				

Table 12 the Temperature for Room Temperature
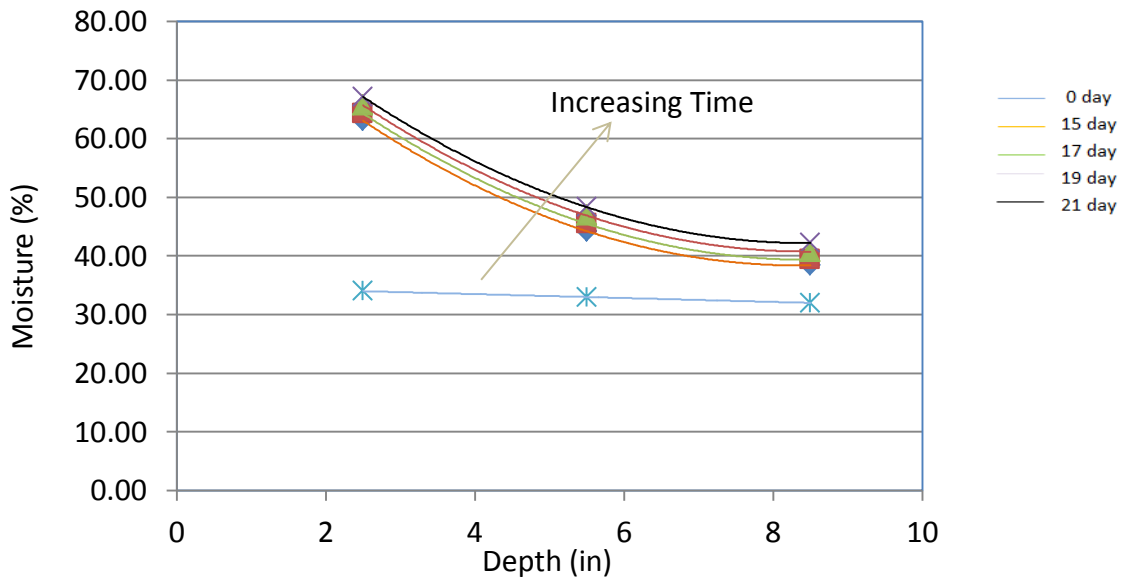
Figure 17 Depths vs. Moisture for 40 ^{o}C

Figure 17 shows the moisture distribution under 40 °C and at different times. Similar trends are seen with the room temperature case. The moisture distribution is higher on the left side which is near the ponding surface. As time increase, the moisture also increases and the tendency is to reach the same value through the specimen. However, for the case of 40 °C, the moisture level is a little higher than those in the case of room temperature.

Time	15 day						
x (in)	2.5	3	3.5	4	4.5	5	5.5
x (mm)	63.5	76.2	88.9	101.6	114.3	127	139.7
H (%)	63.04	59.00	55.33	52.01	49.06	46.46	44.23
Time	17 day						
x (in)	2.5	3	3.5	4	4.5	5	5.5
x (mm)	63.5	76.2	88.9	101.6	114.3	127	139.7
H (%)	64.27	60.26	56.61	53.30	50.35	47.74	45.49
Time	19 day						
x (in)	2.5	3	3.5	4	4.5	5	5.5
x (mm)	63.5	76.2	88.9	101.6	114.3	127	139.7
H (%)	65.67	61.66	58.00	54.69	51.74	49.13	46.88
Time	21 day						
x (in)	2.5	3	3.5	4	4.5	5	5.5
x (mm)	63.5	76.2	88.9	101.6	114.3	127	139.7
H (%)	67.11	63.10	59.44	56.13	53.18	50.57	48.32

Table 13 the Moisture for 40 °C

Time	15 day						
x (in)	2.5	3	3.5	4	4.5	5	5.5
x(mm)	63.5	76.2	88.9	101.6	114.3	127	139.7
T (°C)	29.55	29.34	29.14	28.94	28.74	28.55	28.36
Time	17 day						
x (in)	2.5	3	3.5	4	4.5	5	5.5
x(mm)	63.5	76.2	88.9	101.6	114.3	127	139.7
T (°C)	29.96	29.75	29.55	29.35	29.15	28.96	28.77
Time	19 day						
x (in)	2.5	3	3.5	4	4.5	5	5.5
x(mm)	63.5	76.2	88.9	101.6	114.3	127	139.7
T (°C)	30.43	30.22	30.02	29.82	29.63	29.44	29.25

Time	21 day						
x (in)	2.5	3	3.5	4	4.5	5	5.5
x(mm)	63.5	76.2	88.9	101.6	114.3	127	139.7
T (^{o}C)	31.00	30.79	30.59	30.39	30.19	30.00	29.81

Table 14 the Temperature for 40 ^{o}C
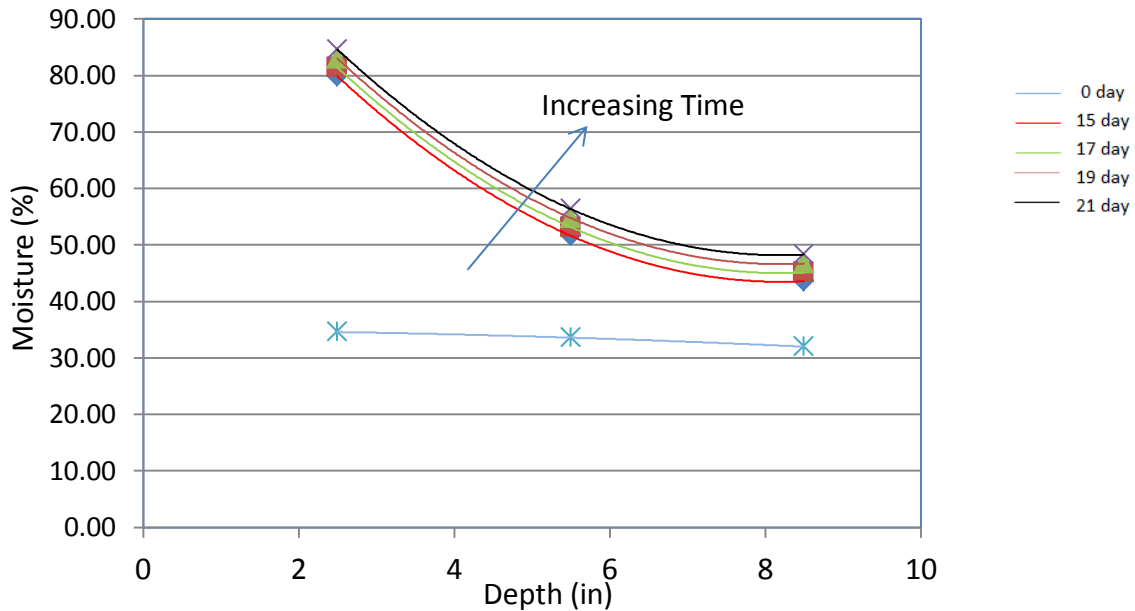
Figure 18 Depths vs. Moisture for 70 ^{o}C

Figure 18 shows the moisture distribution under 70 ^{o}C and at different times. Once again, it displays similar trends as the other two cases. The difference is that the 70 ^{o}C case achieves the highest moisture value in the sample.

Time	15 day						
x (in)	2.5	3	3.5	4	4.5	5	5.5
x (mm)	63.5	76.2	88.9	101.6	114.3	127	139.7
H (%)	79.85	73.74	68.20	63.21	58.79	54.93	51.63
Time	17 day						
x (in)	2.5	3	3.5	4	4.5	5	5.5
x (mm)	63.5	76.2	88.9	101.6	114.3	127	139.7
H (%)	81.40	75.30	69.75	64.77	60.34	56.48	53.17
Time	19 day						
x (in)	2.5	3	3.5	4	4.5	5	5.5
x (mm)	63.5	76.2	88.9	101.6	114.3	127	139.7
H (%)	83.00	76.89	71.35	66.36	61.94	58.07	54.77
Time	21 day						

x (in)	2.5	3	3.5	4	4.5	5	5.5
x (mm)	63.5	76.2	88.9	101.6	114.3	127	139.7
H (%)	84.60	78.49	72.95	67.96	63.53	59.67	56.36

Table 15 the Moisture for 70 ^{o}C

Time	15 day						
x (in)	2.5	3	3.5	4	4.5	5	5.5
x(mm)	63.5	76.2	88.9	101.6	114.3	127	139.7
T (^{o}C)	43.74	43.50	43.28	43.06	42.86	42.67	42.50
Time	17 day						
x (in)	2.5	3	3.5	4	4.5	5	5.5
x(mm)	63.5	76.2	88.9	101.6	114.3	127	139.7
T (^{o}C)	45.03	44.76	44.50	44.25	44.02	43.81	43.61
Time	19 day						
x (in)	2.5	3	3.5	4	4.5	5	5.5
x(mm)	63.5	76.2	88.9	101.6	114.3	127	139.7
T (^{o}C)	46.17	45.94	45.73	45.52	45.32	45.13	44.95
Time	21 day						
x (in)	2.5	3	3.5	4	4.5	5	5.5
x(mm)	63.5	76.2	88.9	101.6	114.3	127	139.7
T (^{o}C)	43.74	43.50	43.28	43.06	42.86	42.67	42.50

Table 16 the Temperature for 70 ^{o}C
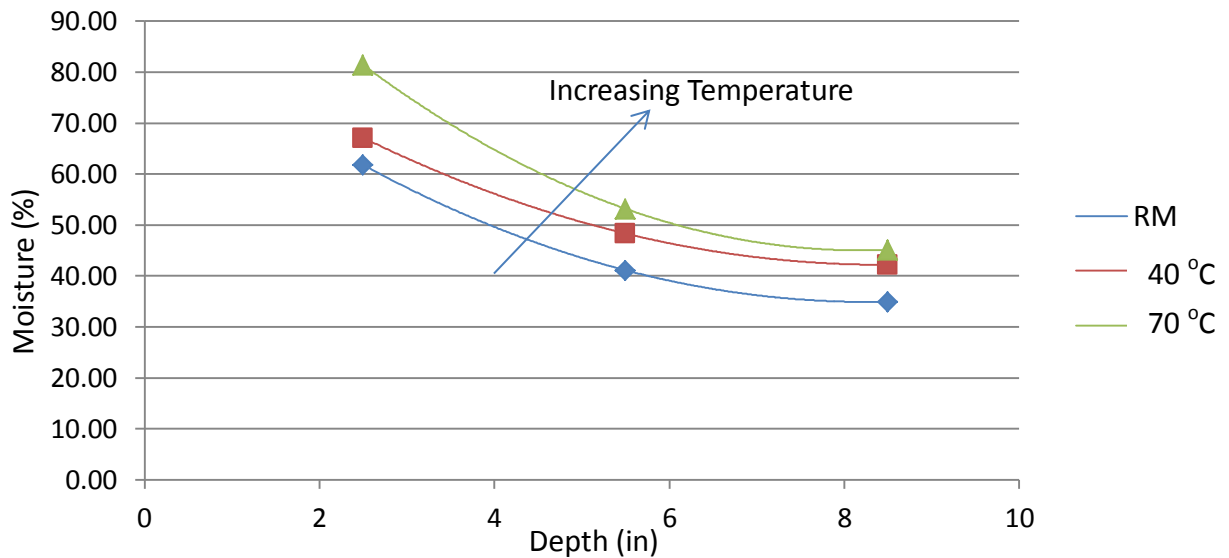
Figure 19 Comparing the Moisture levels under the Same Time and at Different Temperatures

Figure 19 shows the moisture distributions for the three temperature cases and at the same time. Comparing these three curves, 70 °C achieved the highest moisture values and the highest gradient (in the shallow region of the specimens).
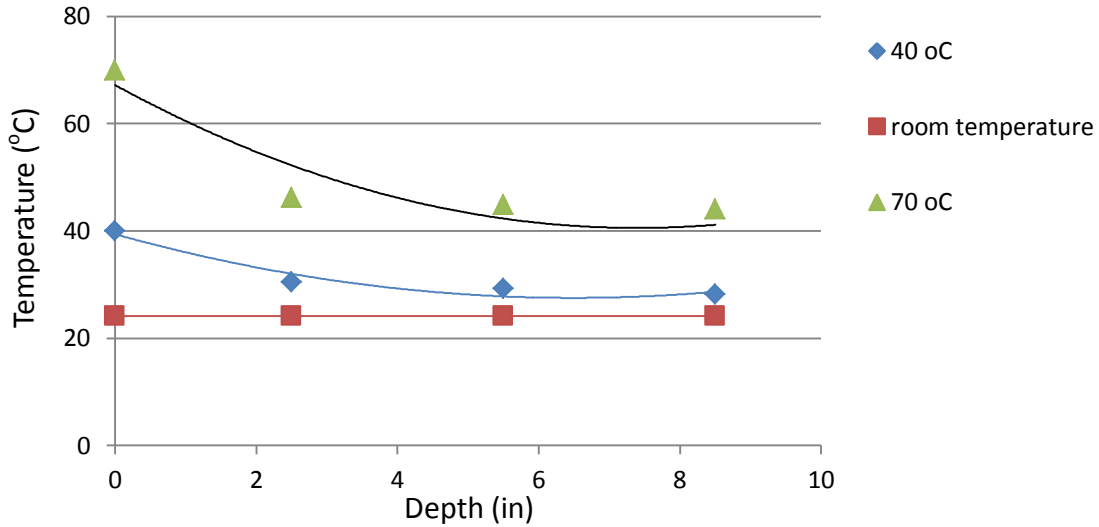
Figure 20 the Temperature Profiles under the Same Time

The Figure 20 shows the temperature profiles for the three temperature cases under the same time. Comparing these three curves, the 70 °C achieved the highest temperature gradient.

4.5 The equation to determine the coupling parameter

In this section, an equation will be derived based on the governing equation, and then it will be used together with the measure data to determine the coupling parameter.

$$\frac{\partial w}{\partial t} = -\nabla \cdot \boldsymbol{J} \qquad (eq\ 4.1)$$

Using the definition of divergence:

$$div(J) = \frac{\partial C}{\partial t} = \frac{A}{V}J \quad (eq\ 4.2)$$

$$V = A \times L \qquad (eq\ 4.3)$$

Combining these two equations:

$$div(J) = \frac{J}{L} \qquad (eq\ 4.4)$$

where:
$L = the\ distance\ between\ two\ adjacent\ points\ on\ a\ concentration\ profile;$
$V = the\ volume\ of\ concrete\ between\ two\ adjacent\ points;$
$A = the\ surface\ area;$

$$\frac{\partial w}{\partial t} = -div(J) = -\frac{J}{L} \quad (eq\ 4.5)$$

$$J = -D_{HH}\ grad\ H - D_{HT}\ gradT \quad (eq\ 4.6)$$

Combining the latest two equations:

$$\frac{\partial w}{\partial t} = -\frac{-D_{HH}\ grad\ H - D_{HT}\ grad\ T}{L} = \frac{D_{HH}\ grad\ H + D_{HT}\ grad\ T}{L} \quad (eq\ 4.7)$$

Rearrange:

$$\frac{\partial w}{\partial H}\frac{\partial H}{\partial t} = \frac{D_{HH}\ grad\ H}{L} + \frac{D_{HT}\ grad\ T}{L} = \frac{D_{HH}\ \Delta H}{L^2} + \frac{D_{HT}\ \Delta T}{L^2} \qquad (eq\ 4.8)$$

where:

$$\frac{\partial w}{\partial H} = the\ moisture\ capacity\ ;$$

For the specimen without the temperature gradient, $\Delta T = 0$, so,

$$\frac{\partial w}{\partial H}\frac{\partial H}{\partial t} = \frac{D_{HH}\ grad\ H}{L} = \frac{D_{HH}\ \Delta H}{L^2} \qquad (eq\ 4.9)$$

In the last two equations, Equations (1) and (2), there are three material parameters, the moisture capacity, the diffusion coefficient, D_{HH}, and the coupling parameter, D_{HT}. The moisture capacity is estimated by an available model (shown below), and the other two are determined using the measured test data. First, D_{HH} is determined using the test data without temperature gradient, and finally the coupling parameter D_{HT} is determined using the test data with the temperature gradient.

Moisture Capacity

Moisture capacity is the derivative of the equilibrium adsorption isotherm. Moisture capacity is related to the water-cement ratio, specimen age, cement type, temperature and humidity. Xi et al. (1994a) developed a model based on BET theory to moisture capacity of concrete. From Figure 21 and Figure 22 (Xi et al. 1994a), it is evident that moisture capacity changes with the water cement ratio and age. In the beginning, the moisture capacity decreases; afterwards, it becomes a constant; and finally increases. The physical meaning of the first transition points in moisture capacity, transferring from the initial drop to the constant region, may correspond to the stage that the moisture in pores has reached the monolayer capacity in adsorption isotherm. The physical meaning of the second turn indicates a transitioning from the constant region to the final increase, which may correspond to the beginning of capillary condensation.
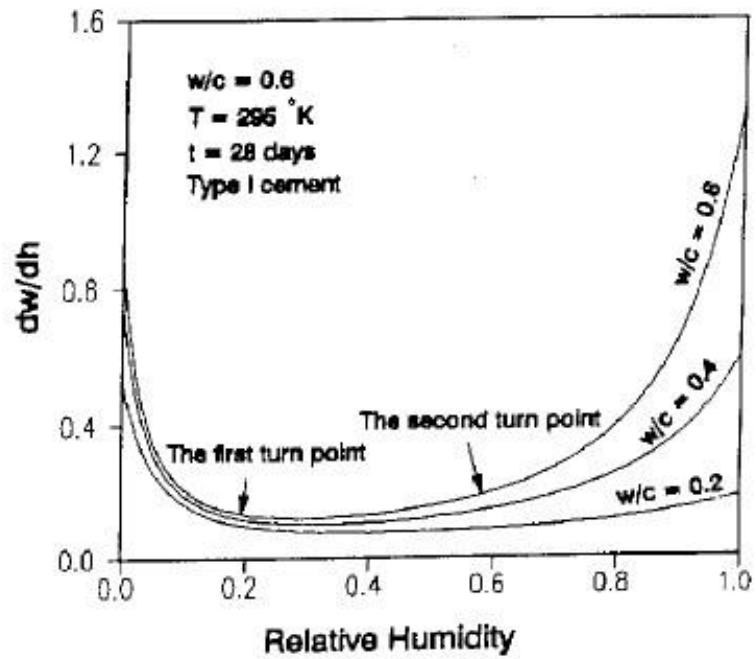
Figure 21 Effect of w/c on Moisture Capacity (Xi et al. 1994a)
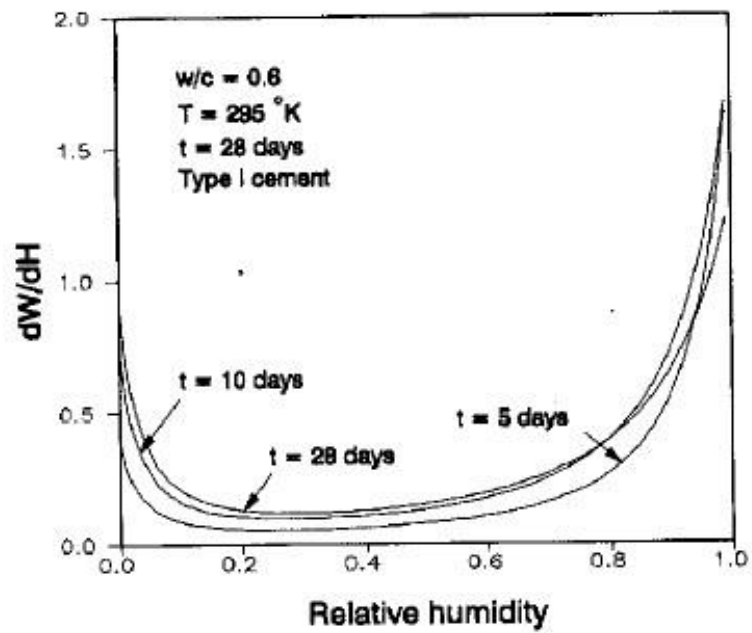

Figure 22 Effect of Age on Moisture Capacity (Xi et al. 1994a)

The moisture capacity can be obtained from the equilibrium adsorption isotherm (Xi et al. 1994a, 1994b):

$$\frac{\partial w}{\partial H} = \frac{CkV_m + wk[1 + (C-1)kH] - wk(1-kH)(C-1)}{(1-kH)[1 + (C-1)kH]} \quad (eq \ 4.10)$$

$$w = \frac{CkV_mH}{(1-kH)[1 + (C-1)kH]} \quad (eq \ 4.11)$$

$$C = exp\left(\frac{E_1 - E_l}{RT}\right) \quad (eq \ 4.12)$$

where:
$H \quad = \ ^p/_{p_s} \ , p_s \ is \ the \ pressure \ at \ saturation;$
$C \ \& \ V_m = the \ constants; \ V_m \ is \ the \ monolayer \ capacity;$
$E_1 \quad = the \ total \ heat \ of \ adsorption \ per \ mole \ of \ vapor;$
$E_l \quad = the \ latent \ heat \ of \ condensation \ per \ mole;$
$R \quad = the \ gas \ constant;$
$T \quad = the \ absolute \ temperature;$
$w \quad = the \ quantity \ of \ vapor \ adsorbed \ at \ pressure \ p \ in \ grams \ of \ water \ per$
$\quad \quad gram \ of \ cement \ paste;$

Note: the adsorption of water in hardened Portland cement paste is affected by many parameters, which contribute to the hydration process of Portland cement and hence to the constitution of the pore structure and pore-size distribution. Factors include: water cement ratio, type of cement, curing time, temperature, curing method, carbonation (for structures with thin cross-section) and added ingredients and aggregates cement ratio. In this study, the variations monitored are water cement ratio and temperature.

Monolayer Capacity

The monolayer capacity, V_m, is defined as the mass of adsorbate required to cover the adsorbent with a single molecular layer. From the observed test data, the empirical expression for V_m can be described as (Xi et al. 1994a):

$$V_m = V(t, w/c, c_t, T) = V_t(t)V_{ct}(c_t)V_{wc}(w/c)V_T(T) \qquad (eq\ 4.13)$$

1. $V_t(t)$ shows the effect of the curing time.

$$V_t(t) = 0.068 - \frac{0.22}{t}, \quad only\ valid\ for\ t \geq 5\ days;$$

$$V_t(t) = 0.024, \quad for\ t \leq 5\ days;$$

2. V_{ct} shows the effect of the various cement types.

$$Type\ 1: V_{ct} = 0.9;\ Type\ 2: V_{ct} = 1;\ Type\ 3: V_{ct} = 0.85;\ Type\ 4: V_{ct} = 0.6;$$

3. V_{wc} shows the effect of the water cement ratio.

$$V_{wc} = 0.85 + 0.45\frac{w}{c}, \qquad for\ 0.3 \leq \frac{w}{c} \leq 0.6;$$

$$V_{wc} = 0.85 + 0.45 \times 0.3 = 0.985, \qquad for\ \frac{w}{c} \leq 0.3;$$

$$V_{wc} = 0.85 + 0.45 \times 0.6 = 1.12, \qquad for\ \frac{w}{c} \geq 0.6;$$

Parameter C

Following the substitution, $C_0 = (E_1 - E_l)/R$

$$C = exp\left(\frac{C_0}{T}\right) \qquad\qquad (eq\ 4.14)$$

Note: at near room temperature the shape of the adsorption curve changes with temperature very slightly, and this means that the isotherms are considered to be insensitive to changes in C within a rather wide range of values. To simplify analysis, the expected value of C_0 can be obtained from the test data: $C_0 = 855$; however, for high

temperatures these assumptions are not valid and other phenomena need be taken into consideration.

Parameter k

Parameter k is obtained from the assumption that the number of adsorbed layers is finite. In order to determine k, first the expression for the number of adsorbed layers at the saturation state, n, must be obtained. Afterwards, n is converted into k:

$$n = N(t, w/c, T) = N_t(t) \, N_{wc}(w/c) \, N_{ct}(c_t) \, N_T(T) \qquad (eq\ 4.15)$$

$$N_t(t) = 2.5 + \frac{15}{t} \, , for\ t > 5; otherwise\ N_t(t) = 5.5$$

$$N_{wc}(w/c) = 0.33 + 2.2\frac{w}{c}$$

$$Type\ 1: N_{ct} = 1.1; \ Type\ 2: N_{ct} = 1; \ Type\ 3: N_{ct} = 1.15; \ Type\ 4: N_{ct} = 1.5;$$

$$k = \frac{\left(1 - \frac{1}{n}\right)C - 1}{(C - 1)} \qquad 0 < k < 1 \qquad\qquad (eq\ 4.16)$$

The model for moisture capacity

The variations of V_m affected by temperature are only due to the thermal expansion or contraction of the adsorbed layer. The volumetric changes of the adsorbate water are very small at room temperature. Therefore, V_T may be equal to 1. In fact, empirical evidence shows that for moderate changes in temperature, the variation of n is negligible. Therefore, V_T may also be equal to 1 as well. However, for temperature much higher than room temperature, especially above 100 ^{o}C, further phenomena occur and a more complex model, based on the thermodynamic properties of water, is required.

In general, the model and final formulas for V_m, C and k are as follows:

$$w = \frac{CkV_mH}{(1-kH)[1+(C-1)kH]}$$

$$V_m = \left(0.068 - \frac{0.22}{t}\right)\left(0.85 + 0.45\frac{w}{c}\right)V_{ct}$$

$$t > 5\ days, \qquad 0.3 < w/c < 0.7$$

$$Type\ 1: V_{ct} = 0.9;\ Type\ 2: V_{ct} = 1;\ Type\ 3: V_{ct} = 0.85;\ Type\ 4: V_{ct} = 0.6;$$

$$For: t \le 5\ days,\ \ set\ t = 5\ days;$$

$$For: w/c \le 0.3,\ \ set\ w/c = 0.3;$$

$$For: w/c \ge 0.7,\ \ set\ w/c = 0.7;$$

$$C = exp\left(\frac{C_0}{T}\right),\ \ C_0 = 855$$

$$k = \frac{\left(1 - \frac{1}{n}\right)C - 1}{(C-1)}$$

$$n = \left(2.5 + \frac{15}{t}\right)\left(0.33 + 2.2\frac{w}{c}\right)N_{ct}$$

$$t > 5\ days, \qquad 0.3 < w/c < 0.7$$

$$Type\ 1: N_{ct} = 1.1;\ Type\ 2: N_{ct} = 1;\ Type\ 3: N_{ct} = 1.15;\ Type\ 4: N_{ct} = 1.5;$$

$$For: t \le 5\ days,\ \ set\ t = 5\ days;$$

$$For: w/c \le 0.3,\ \ set\ w/c = 0.3;$$

$$For: w/c \ge 0.7,\ \ set\ w/c = 0.7;$$

4.6 The coupling parameter obtained based on the present test data

Frist of all, the moisture capacity for three cases, room temperature, 40 $^{\circ}$C and 70 $^{\circ}$C were calculated and shown in Tables 17, 18, and 19 Then, from the equation 4.17 for the isothermal condition, we can obtain equation 4.18

$$\frac{dw}{dH}\frac{dH}{dt} = \frac{D_{HH}\,\Delta H}{L^2} \qquad\qquad (eq\ 4.17)$$

$$D_{HH} = \frac{dw}{dH}\frac{dH}{dt}\frac{L^2}{\Delta H} \qquad\qquad (eq\ 4.18)$$

D_{HH} can be determined using equation 4.18 together with the model prediction for moisture capacity and the test data from the isothermal condition (under the room temperature). The results are shown in Table 20, and the unit for D_{HH} is (inch^2/sec).

Finally, from the equation 4.19 for 40 ^{o}C and 70 ^{o}C cases, we can obtain equation 4.20

$$\frac{dw}{dH}\frac{dH}{dt} = \frac{D_{HH}\,\Delta H}{L^2} + \frac{D_{HT}\,\Delta T}{L^2} \qquad\qquad (eq\ 4.19)$$

$$D_{HT} = \left(\frac{dw}{dH}\frac{dH}{dt} - \frac{D_{HH}\,\Delta H}{L^2}\right)\frac{L^2}{\Delta T} \qquad\qquad (eq\ 4.20)$$

D_{HT} can then be determined using equation (d) together with the model prediction for moisture capacity, the parameter D_{HH}, and the test data from 40 ^{o}C and 70 ^{o}C cases. The results are shown in Table 21 for the case of 40 ^{o}C and Table 22 for the case of 70 ^{o}C. The unit for D_{HT} is (%·in^2/sec/Celsius).

Note: In this experiment, the distribution just occurred in one direction. Therefore, the equation here uses the total differential. It should be noted that L is the length between the two adjacent points and is equal to 0.5 inches.

Moisture capacity for room temperature case						
x (in)	2.5	3	3.5	4	4.5	5	5.5
x(mm)	63.5	76.2	88.9	101.6	114.3	127	139.7
15d	0.19	0.17	0.16	0.15	0.14	0.13	0.13
17d	0.20	0.18	0.16	0.15	0.14	0.14	0.13
19d	0.20	0.18	0.16	0.15	0.14	0.14	0.13
21d	0.21	0.19	0.17	0.16	0.15	0.14	0.14

Table 17 the Moisture Capacity (%/%) for Room Temperature

Moisture capacity for 40 oC case							
x (in)	2.5	3	3.5	4	4.5	5	5.5
x(mm)	63.5	76.2	88.9	101.6	114.3	127	139.7
0d	0.21	0.19	0.17	0.16	0.15	0.14	0.14
2d	0.22	0.20	0.18	0.17	0.16	0.15	0.14
4d	0.23	0.20	0.18	0.17	0.16	0.15	0.15
6d	0.24	0.21	0.19	0.18	0.16	0.16	0.15

Table 18 the Moisture Capacity (%/%) for 40 ^{o}C

Moisture capacity for 70 oC case							
x (in)	2.5	3	3.5	4	4.5	5	5.5
x(mm)	63.5	76.2	88.9	101.6	114.3	127	139.7
0d	0.37	0.30	0.25	0.21	0.19	0.17	0.16
2d	0.40	0.31	0.26	0.22	0.20	0.18	0.17
4d	0.42	0.33	0.27	0.23	0.20	0.19	0.17
6d	0.45	0.35	0.29	0.24	0.21	0.19	0.18

Table 19 the Moisture Capacity (%/%) for 70 ^{o}C

x (in)	2.5-3	3-3.5	3.5-4	4-4.5	4.5-5	Average
D_{H-H} 2d	3.75E-03	3.73E-03	3.83E-03	4.05E-03	4.43E-03	3.96E-03
D_{H-H} 4d	4.97E-03	4.82E-03	4.82E-03	4.96E-03	5.27E-03	4.97E-03
D_{H-H} 6d	5.17E-03	5.30E-03	5.52E-03	5.87E-03	6.35E-03	5.64E-03

Table 20 the Coefficient D_{HH} (inch^2/sec)

x (in)	2.5-3	3-3.5	3.5-4	4-4.5	4.5-5	5-5.5	Average
D_{H-T} 2 d	3.44E-04	3.34E-04	3.39E-04	3.56E-04	3.81E-04	4.14E-04	3.61E-04
D_{H-T} 4 d	3.19E-04	2.90E-04	2.90E-04	3.13E-04	3.54E-04	4.11E-04	3.30E-04
D_{H-T} 6 d	2.76E-04	2.48E-04	2.52E-04	2.80E-04	3.28E-04	3.93E-04	2.96E-04

Table 21 the Coefficient D_{HT} (%·in2/sec/Celsius) for 40 ^{o}C

x (in)	2.5-3	3-3.5	3.5-4	4-4.5	4.5-5	5-5.5	Average
$D_{H\text{-}T}$ 2 d	7.66E-04	5.93E-04	5.04E-04	4.74E-04	4.91E-04	5.48E-04	5.63E-04
$D_{H\text{-}T}$ 4 d	8.39E-04	5.95E-04	4.71E-04	4.26E-04	4.39E-04	4.99E-04	5.45E-04
$D_{H\text{-}T}$ 6 d	7.59E-04	5.09E-04	3.82E-04	3.41E-04	3.64E-04	4.42E-04	4.66E-04

Table 22 the Coefficient D_{HT} (%·in2/sec/Celsius) for 70 ^{o}C

Comparing these two tables, Tables 21 and 22, the coefficient D_{HT} for 70 ^{o}C is a little higher than that of 40 ^{o}C case, which means the coupling parameter may be temperature dependent.   In general, for the moisture transport under non-isothermal condition, the moisture concentration of course plays the major role while the coupling effect should be also considered. What's more, the coupling parameter, D_{HT}, is related with the temperature. If the temperature is higher, the coupling effect is more significant.

CHAPTER 5

CONCLUSIONS AND RECOMMENDATIONS

Conclusions

1. A literature review was performed on the coupling effects between heat transfer and moisture transport in concrete, including the effect of heat transfer on moisture transport, the so-called Soret effect, and the effect of moisture transport on heat transfer, the so-called Dofour effect. Although the two coupling effects were recognized some time ago and studied for other materials, there has been no systematic study for concrete.

2. A case study was found in the literature and it was provided to show the moisture transport and heat transfer in concrete at elevated temperatures. Under high temperatures, in addition to the coupling effects, phase transformation of water into vapor in concrete pores must be considered and the high vapor pressure may cause spalling damage of the concrete. Formulation of the governing equations, finite element solutions, and experimental study of the concrete under high temperature were reviewed.

3. An experimental technique was established for understanding the temperature effect on moisture transport in concrete. The technique was used for studying the moisture penetration into concrete with and without temperature gradient. The test data showed that the effect of temperature gradient is significant and should be considered in the analysis of moisture transport in concrete under non-isothermal condition.

4. Governing equations were established for the moisture transport taking into account the effect of temperature gradient, and for the heat transfer taking into account the moisture effect. In the two governing equations, the gradient of pore relative humidity, H, was

used as one of the basic driving forces for the moisture transport in concrete under isothermal condition. The other driving force is the gradient of temperature T.

5. An analysis method was developed based on the governing equations to calculate the moisture diffusion coefficients D_{HH}, and the coupling parameter D_{HT} (for the Soret effect). Using the present experimental results, the two transport parameters were evaluated.

Recommendations

1. This study focused on the evaluation of the Soret effect. Future studies should be done for the Dufour effect.

2. The number of specimens used in the present study was very limited. More systematic research should be conducted to study the effect of concrete mix design and additives on the coupling parameters.

BIBLIOGRAPHY

Anold, J.R., Garrabrants, A.C., Samson, E., Flach, G.P., and Langton, C.A. (2009) "Moisture Transport Review", *Cementitous Barriers Partnership,* CBP-TR-2009-002, Rev.0.

Bazant, Z.P., M.ASCE and Thonguthai, W. (1978) "Pore Pressure and Drying of Concrete at High Temperature", *Journal of the Engineering Mechanics Division,* Vol. 104, No.5, 1059-1079.

Bazant, Z.P., and Thonguthai, W. (1979) "Pore Pressure in heated concrete walls: theoretical prediction." *Magazine of Concrete Research,* Vol.31, No. 107, 67-76.

Bazant, Z.P., and Wittmann, F.H. (1982) "Creep and Shrinkage in Concrete Structures" *JOHN WILEY & SONS,* Chapt. VII, 163-256.

Bazant, Z.P., (1975) "Theory of Creep and Shrinkage in Concrete Structures: A Précis of Recent Development." *Reprinted from Mechanics Today, Vol.2, ed. By S. Nemat-Nasser, Pergamon Press,* Chapt. I, 1-93.

Bazant, Z.P., Chern, J. and Thonguthai, W. (1981) "Finite Element Program for Moisture and Heat Transfer in Heated Concrete." *Nuclear Engineering and Design,* 68, 61-70.

Bary, B., Morais, M.V.G., Poyet, S. and Durand, S. (2012) "Simulations of the Thermo-hydro-mechanical Behavior of an Annular Reinforced Concrete Structure Heated up to 200 $^{\circ}$C" *Engineering Structure,* 36, 302-315.

Bertolini, L., Elsener, B., Pedeferri, P., and Plder, R. (2004) "Corrosion of Steel in Concrete." *Wiley-VCH Verlag Gmbh & Co. KGaA, Weinheim,* 28, 49, 91.

Dayan, A. and Gluekler, E.L. (1981) "Heat and Mass Transfer within an Intensely Heated Concrete Slab." *Int. J. Heat Mass Transfer,* Vol. 25, No.10, 1461-1467.

Huang, C.L.D., Siang, H.H. and Best, C.H. (1979) "Heat and Moisture Transfer in Concrete Slabs." *Int. J. Heat Mass Transfer,* Vol. 22, 257-266.

Han, B., Yang, Z., Shi, X. and Yu, X. (2012) "Transport Properties of Carbon-Nanotube/Cement Composites", *Journal of Materials Engineering and Performance,* Vol. 22(1), 184-189.

Haupl, J., and Fechner, H. (1996) "Coupled Heat Air and Moisture Transfer in Building Structures", *Int. J. Heat Mass Transfer* Vol. 40, No. 7, 1633-1642.

Harstad, K. (2009) "Modeling the Soret Effect in Dense Media Mixtures", *Ind. Eng. Chem. Res.* 48, 6907-6915.

Isteita, M.H. (2009) "The Effect of Thermal Conduction on Chloride Penetration in Concrete" *Faculty of the Graduate School of the University of Colorado.*

Kim, K., Jeon, S., Kim, J. and Yang, S. (2002) "An Experimental Study on Thermal Conductivity of Concrete." *Cement and Concrete Research,* 33, 363-371.

Lv, X. (2002) "Modeling of Heat and Moisture Transfer in Buildings I. Model Program" *Energy and Buildings,* 34, 1033-1043.

Platten, J.K. (2006) "The Soret Effect: A Review of Recent Experimental Results." *Journal of Applied Mechanics,* 73, 5-15.

Szekeres, A. (2012) "Cross-Coupled Heat and Moisture Transport" *Journal of Thermal Stresses,* 35: 248-268.

Xi, Y., Bazant, Z.P. and Jennings, H.M. (1994a) "Moisture Diffusion in Cementitou Materials: Adsorption Isotherm." *Advancement Cement Based Materials,* 1,248-257.

Xi, Y., Bazant, Z.P. and Jennings, H.M. (1994b) "Moisture Diffusion in Cementitou Materials: Moisture Capacity and Diffusivity." *Advancement Cement Based Materials,* 1,258-266.

Zhong, Z., and Braun, J.E. (2008) "Combined Heat and Moisture Transport Modeling for Residential Building." *U.S. National Institute of Standards and Technology,* 1-14.

APPENDIX A

A total of three 3×6" concrete cylinders were casted and de-molded after 24 hours. Then they were left to cure in the curing room. Three cylinders had the same mix design. After curing, all specimens were capped. A compression test was conducted using an MTS load frame. The program controlled displacement control at a rate of 0.0005 in/sec:

Sample #	#1	#2	#3
Peak Load (kip)	27.83	24.79	24.93
Area (in^2)	7.07	7.07	7.07
fc' (ksi)	3.94	3.51	3.53

Table 23 Compression Test Results